



Published in final edited form as:

Dev Dyn. 2022 July ; 251(7): 1175–1195. doi:10.1002/dvdy.456.

Hedgehog (HH) pathway endogenous antagonist HHIP: unique lingual expression in filiform papillae during homeostasis and ectopic in fungiform papillae during HH signaling inhibition

Archana Kumari^{1,2}, Libo Li¹, Alexandre N. Ermilov³, Nicole E. Franks⁴, Andrzej A. Dlugosz^{3,4}, Benjamin L. Allen^{4,*}, Charlotte M. Mistretta^{1,*}

¹Department of Biologic and Materials Sciences, School of Dentistry, University of Michigan, Ann Arbor, Michigan, United States of America

²Cell Biology and Neuroscience, Rowan University School of Osteopathic Medicine, Stratford, New Jersey, United States of America

³Department of Dermatology, Michigan Medicine, Ann Arbor, Michigan, United States of America

⁴Department of Cell and Developmental Biology, University of Michigan Medical School, Ann Arbor, Michigan, United States of America

Abstract

Background: Hedgehog (HH) signaling is essential for homeostasis in gustatory fungiform papillae (FP) and taste buds. However, activities of HH antagonists in these tissues remain unexplored. We investigated a potential role for HH-interacting protein (HHIP), an endogenous pathway antagonist, in regulating HH signaling during taste organ homeostasis. We found a restricted pattern of *Hhip*-expressing cells in the anterior epithelium of each nongustatory filiform papilla (FILIF) only. To test for roles in antagonism of HH signaling, we investigated HHIP after pathway inhibition with SMO inhibition via sonidegib and *Smo* deletion, *Gli2* deletion/suppression, or with chorda tympani/lingual nerve cut.

Results: In all approaches, the HHIP expression pattern was retained in FILIF suggesting HH-independent regulation of HHIP. Remarkably, after pathway inhibition, HHIP expression was detected also in the conical, FILIF-like atypical FP. We found a close association of *de novo* expression of HHIP in atypical FP with loss of *Gli1+*, HH-responding cells. Further, we report that PTCH1 is another potential HH antagonist in FILIF that co-localizes with HHIP.

*Co-corresponding authors Charlotte M. Mistretta, cmist@umich.edu (CMM), Telephone: 734-647-3911 (CMM), Please contact BLA for any queries. Benjamin L. Allen, benallen@umich.edu (BLA), 734-615-7512 (BLA).

Data availability statement: All data generated or analyzed during this study are included in this published article.

Ethics approval statement: The study was conducted according to the guidelines of the National Institutes of Health and approved protocols of the University of Michigan Institutional Animal Care and Use Committee.

Patient consent statement: Not applicable

Permission to reproduce material from other sources: Not applicable

Conflicts of Interest: The authors declare no conflict of interest.

Conclusions: After HH pathway inhibition the ectopic expression of HHIP correlates with a FILIF-like morphology in atypical FP and we propose that localized expression of the HH antagonist HHIP regulates pathway inhibition to maintain FILIF during tongue homeostasis.

Keywords

taste bud; Hedgehog interacting protein; Hedgehog antagonist; Sonidegib; *Ptch1*; chorda tympani nerve

Introduction

Hedgehog (HH) signaling is a principal regulator of taste organ maintenance, renewal and regeneration.¹⁻⁹ This essential role for HH signaling has been demonstrated using pharmacologic and genetic models of HH pathway disruption, which have revealed taste bud (TB) loss in fungiform papillae (FP), the circumvallate papilla (CV) and the soft palate of mouse and rat.²⁻⁵ However, the lingual non-taste filiform papillae (FILIF) that are essential in food bolus manipulation are not noticeably affected. Instead, during HH pathway disruption, FP acquire a conical, heavily keratinized apex and morphology similar to FILIF.⁸ Whereas there is a broad understanding of HH regulation in taste homeostasis, there is no clarity about roles for this pathway in pattern maintenance in the anterior tongue gustatory FP organs versus nongustatory FILIF organs. Since patients who use HH pathway inhibiting drugs experience taste disturbances, in-depth knowledge of HH pathway regulation of lingual organs is crucial for clinical understanding of taste disruption.⁹

The HH pathway includes two core canonical membrane components, Patched 1 (PTCH1) and Smoothened (SMO).¹⁰ In the absence of HH ligand, PTCH1 inhibits SMO and the pathway is inactive. In the adult tongue, HH signaling is initiated through Sonic HH (SHH) ligand binding to PTCH1 that relieves SMO inhibition. SMO then mediates a signal transduction cascade leading to modulation of GLI transcription factor activity and expression of target genes including *Gli1*, which is both a pathway component and a transcriptional target. Based on the expression of HH-producing (SHH+) and HH-responding (*Gli1*+) cells, it has been suggested that HH signaling is active within FP and TB, but inactive in FILIF.^{8,9} On the other hand, *Gli2*-expressing cells are present in both FP and FILIF,^{2,6,8} and comparison of *Gli1* and *Gli2* expression suggests that there is distinctive HH signaling within the FP and FILIF lingual organ types.⁹

During taste organ homeostasis, SHH ligand is expressed in TB and nerves in FP.¹⁻⁷ HH-responding, *Gli1* + cells are found bracketing the TB and in basal cells of the FP, positioned to respond via paracrine signaling to SHH from the TB.⁶ Notably, the non-taste FILIF do not express SHH or *Gli1*. Whereas several HH pathway components have been localized in the tongue and FP/TB,⁸ expression patterns of HH pathway antagonists remain largely unexplored.

Hedgehog-interacting protein (HHIP) is a vertebrate-specific, HH-binding, cell surface-associated receptor that functions as an endogenous antagonist of HH signaling in many organs.¹¹⁻¹⁶ However, this antagonist has not been studied in the adult tongue or taste system. *Hhip*, along with *Ptch1* and *Ptch2*, are transcriptional targets that are generally

induced in response to active HH signaling.^{12,14,17–19} HHIP, PTCH1 and PTCH2 all bind and sequester HH ligands, altering the balance between bound and unbound PTCH1, allowing for the re-establishment of PTCH1-dependent repression of SMO.^{14–16} Thus, HH-dependent transcriptional up-regulation of *Hhip*, *Ptch1*, and *Ptch2* provides a negative feedback mechanism to control the levels of HH signaling. However, potential roles for these signaling antagonists in taste organ regulation have not been studied.

We have investigated the potential for endogenous HH pathway feedback in the control of taste organ homeostasis. We studied FP, CV, and foliate papillae (FOL) on the posterior lateral tongue. Specifically, we characterized *Hhip* expression using a *Hhip^{lacZ}* mouse, and also established HHIP protein localization in lingual FILIF papillae. We also investigated HHIP lingual distributions during HH pathway inhibition with: 1) the pharmacologic SMO antagonist sonidegib, 2) epithelial *Smo* deletion, 3) epithelial *Gli2* deletion, and 4) epithelial expression of a *Gli2* repressor. Remarkably, in all cases, HH signaling disruption induces aberrant expression of HHIP in the FP apex, where it is typically not present, concomitant with the altered appearance of FP. Cutting the chorda tympani and lingual nerves that innervate FP also results in ectopic *Hhip* expression in morphologically altered FILIF-like FP, similar to pharmacological and genetic blockade of HH signaling. Notably, in all models of HH pathway disruption, HHIP expression in FILIF remains unaltered. We also identified similar ectopic *Ptch1* expression following HH pathway inhibition. Based on these results, we propose a model whereby *Hhip* and *Ptch1* are expressed in a HH-independent fashion in non-taste FILIF to restrain HH pathway activity in these organs and thus restrict HH signaling to taste FP.

Results

Expression of HH pathway components in the tongue

Active HH signaling requires HH ligands, PTCH1-SMO signal transduction, and the GLI transcription factors (Figure 1A–A’).¹⁰ HHIP controls HH pathway activity by binding to secreted HH ligands.¹² We compared expression of HH pathway components in the adult tongue, a complex lingual organ with taste and non-taste papillae.

HH pathway activity, indicated by whole tongue X-Gal staining in *Gli1^{lacZ}* reporter mice, was observed in FP, CV and Foliate taste papillae (FOL), but not in non-taste FILIF organs (Figure 1B–B’’) whereas the main transcriptional activator, *Gli2*, was more broadly expressed in all taste papillae and non-taste FILIF (Figure 1C–C’). Similar to *Gli2*, *Ptch1* expression was distributed in all gustatory papillae (FP, CV, FOL) and in non-taste FILIF in the intermolar eminence (Figure 1D–D’’) where staining was less intense.

Hhip, like *Gli1*, is a direct transcriptional target of the HH pathway.^{17–19} Although HHIP is involved in homeostatic functions in other tissues,²⁰ *Hhip* expression in the tongue has not been investigated. Strikingly, and distinct from *Gli1*, *Hhip* expression is not observed in any taste papillae (FP, CV, FOL), but is expressed within FILIF in the anterior tongue and intermolar eminence (Figure 1E–E’’).

In sectioned tongues we confirmed *Hhip* expression location, comparing hematoxylin and eosin (Figure 2A–A'') with X-Gal staining in reporter mice. *Hhip* is not expressed in the apical TB in FP, in epithelial cells surrounding the TB, or in basal epithelial cells of the papilla wall (Figure 2B). The CV and FOL papillae have hundreds of TB in the epithelium of papilla walls and do not have surrounding FILIF (Figure 2A'–A''); in these posterior tongue TB and papillae *Hhip* was not detected (Figure 2B'–B'').

Given that HHIP is a secreted HH pathway antagonist,¹³ we investigated the distribution of HHIP protein in the adult tongue using an antibody.¹³ Notably, we found that HHIP expression matches that of *Hhip*, localizing to FILIF, but absent in lingual FP (Figure 2C), CV (Figure 2C'), and FOL papillae (Figure 2C'').

In addition to the tongue, the soft palate is an oral taste organ^{21,22} where TB are not in specialized papillae, but rather distributed in rows (Figure 3). The soft palate has *Gli1* expression in perigemmal TB cells, basal epithelial cells and stroma beneath TBs (Figure 3B, **inset**). Notably, there is no detectable *Hhip* (gene or protein) expression in epithelium or TB (Figure 3B,C). Thus, neither *Hhip* nor HHIP is present in any of the taste papillae (FP, CV or FOL) or in the soft palate. Instead, *Hhip* expression is apparently unique to lingual nongustatory FILIF.

Distinct HH pathway component expression patterns in anterior tongue FP and FILIF

Because *Hhip* is not detected in the posterior taste papillae or soft palate, we focused further analysis on FP and the surrounding FILIF in the anterior tongue, using X-Gal staining to report *lacZ* expression (Figure 4 **FP, FILIF**). A *lacZ* negative Control demonstrates no background X-Gal staining (Figure 4A,A'). The transcription factors *Gli1* and *Gli2* have overlapping expression in perigemmal TB cells and basal cells in the FP walls (Figure 4B,C). However, unlike *Gli1* (Figure 4B'), *Gli2* expression extends beyond the FP throughout basal epithelial cells of the FILIF (Figure 4C'). *Ptch1* is expressed within the FP epithelial cells surrounding the TB and in papilla basal epithelial cells (Figure 4D); although less apparent in whole tongue imaging, *Ptch1* is also expressed within FILIF (Figure 4D'; cf. Figure 1D,D'). Notably, *Hhip* expression is distinctive; that is, *Hhip* is not expressed in FP (Figure 4E), but is detected in non-taste FILIF (Figure 4E'). Within FILIF there is apparent overlap between *Ptch1* and *Hhip* (Figure 4D',E').

HH pathway antagonists are expressed in the anterior face of FILIF

To more precisely determine the cellular locations for *Hhip* and *Ptch1* expression, we examined specific compartments of the FILIF. The non-gustatory FILIF are distributed across the anterior tongue and in the intermolar eminence (Figure 1B–E). The FILIF structure is distinctive with a cornified keratin spine, anterior and posterior faces, and inter-papilla buttress columns^{23–25} (Figure 5A–A'). The anterior-facing suprabasal cells have dense keratohyalin granules in granular cell layers. Posterior-facing cells are elongated and oriented differently from anterior cells. Inter-papilla, buttress columns bridge the tissue between FILIF, or between FP and FILIF. *Hhip* is expressed in a distinct and restricted fashion in each FILIF, in the basal epithelium and extending through the suprabasal cells in the anterior epithelial face of the papillae (Figure 5,B'). Noticeably, *Hhip* is not expressed

in the FILIF posterior face or in the buttress columns. HHIP expression directly matched *Hhip^{lacZ}* distribution (Figure 5B'').

We compared *Hhip^{lacZ}* cellular localization in the FILIF with other HH signaling components (Figure 5C–F). *Gli1* is not expressed within any of the FILIF (Figure 5C), whereas *Gli2* is throughout the basal epithelial cells (Figure 5D). On the other hand, *Ptch1* (Figure 5E) and *Hhip* (Figure 5F) expressions are comparable, within the anterior face of the FILIF although *Ptch1^{lacZ}* apparently labels fewer cells than *Hhip^{lacZ}* (Figure 5G–G''). Thus, expression of the HH signaling antagonists *Ptch1* and *Hhip* is localized specifically within basal and suprabasal cells at the anterior face of FILIF where there is no expression of *Gli1* or *Gli2* transcription factors. Notably, we cannot exclude the possibility that the apparent suprabasal *Hhip^{lacZ}*₊ and *Ptch1^{lacZ}*₊ cells are actually basal cells running along the shaft of the papilla, which may have stem cell properties.

Ectopic HHIP expression in FP after HH pathway inhibition (HPI)

Hhip is a transcriptional target of the HH pathway.^{12,14,17–19} However, the lack of *Gli* expression in *Hhip*-expressing cells raises the question of whether *Hhip* is expressed in a HH-dependent fashion in the tongue. To test this, we used two approaches to suppress SMO and inhibit HH pathway activity: pharmacologically, with the drug sonidegib (SMO inhibition, Sonidegib), and genetically via epithelial signaling blockade by epithelial-specific *Smo* deletion (epi-*Smo* deletion, *cSmoKO*). We also targeted *Gli2* in the epithelium (epi-*Gli2* deletion, *cGli2KO*; epi-*Gli2* repression, *cGli2 C4*; Figure 6). Hematoxylin and eosin staining was used to define three FP/TB types as the basis for assessing effects^{2–5} (Figure 6A–A''): (I) Typical FP/TB, the FP has a rectangular outline with an oval collection of taste cells, the TB, at the apex (Figure 6A); (II) Atypical FP/TB, the papilla is misshapen at the apex with a reduced number of TB cells (Figure 6A'); (III) Atypical FP/No TB, the papillae acquire a conical, cornified apex, without any apparent TB cells, and a resemblance to FILIF (Figure 6A''). Similar to our previous work, all four models result in a virtual elimination of Typical FP/TB and a substantial increase in Atypical FP/TB and Atypical FP/No TB.^{2–4}

In all control lingual tissue, HHIP expression was observed in each FILIF but not in the FP (Figure 6B–E). Surprisingly, after HPI with pharmacologic SMO inhibition (Sonidegib), or with epithelial-specific *Smo* deletion (*cSmoKO*), not only was *Hhip* expression retained in FILIF, but we also detected ectopic HHIP next to TB remnants in Atypical FP/TB (II) (Figure 6B',C') and in the FP apex in Atypical FP/No TB (III) (Figure 6B'',C''). In Atypical FP/TB (II), HHIP expression bracketed TB remnants on either or both sides (Figure 6B', **arrows**). In Atypical FP/No TB (III), HHIP expression was within the former TB-bearing epithelium (Figure 6B'', **arrow**).

In two other genetic models² that targeted *Gli2* in the epithelium by conditional deletion (epi-*Gli2* deletion), or by expression of a dominant-negative GLI repressor (epi-*Gli2* repression), we detected ectopic HHIP expression in the FP apex in Type II Atypical FP/TB (Figure 6D',E') or Type III Atypical FP/NoTB (Figure 6D'',E''). Notably, in all four models of HH signaling inhibition HHIP expression within FILIF was retained and the ectopic expression effects in FP were similar (Figure 6B'–E', B''–E'').

To investigate the timing of the appearance of ectopic HHIP, we evaluated expression in a mouse model with whole body *Smo* deletion (Figure 7A–C). The TB cell marker K8 was used to identify three FP/TB types. After five days of *Smo* deletion, 61% of all remaining FP were Typical FP/TB and HHIP expression was not seen within these Typical FP/TB. On the other hand, in Atypical FP, with or without TB remnants (39% of all FP), ectopic HHIP expression was detected in the FP apex. Importantly, HH pathway activity, seen with *Gli1lacZ*⁺ cells, was inhibited after five days of whole body *Smo* deletion in all three FP/TB types (Figure 7A'–C'), whereas only the Atypical FP had ectopic HHIP expression (Figure 7B,C). Thus, while the onset of HHIP expression after *Smo* deletion is rapid and correlated with loss of TB cell and associated SHH, it does not appear to be a direct transcriptional response to HH pathway inhibition.

To investigate whether the ectopic HHIP expression in FP is reversible, we examined expression following the cessation of pharmacologic HH pathway inhibition. We reported previously that only a subset of FP/TB recover after withdrawing sonidegib treatment (about 55%).⁴ To establish whether HHIP expression still associates with the FP that do not recover a typical phenotype, we studied HHIP at 14 days of recovery from treatment for 16 days with sonidegib (Figure 7D–F). At 14 days of recovery after Vehicle treatment HHIP was within FILIF only (Figure 7D). Similarly, at recovery from 16 days of sonidegib treatment, the Type I Typical FP/TB (about 50% of all FP) had HHIP in FILIF only; there was no ectopic expression (Figure 7E). However, the remaining Atypical FP/No TB (Type III) (about 40% of all FP) retained ectopic HHIP expression (Figure 7F). During Recovery, HH signaling as indicated by *Gli1lacZ* remain unaltered in Vehicle (Figure 7G) and resumed only in recovered type I, Typical FP/TB of sonidegib cessation group (Figure 7H). These Atypical FP with no TB (and therefore no SHH ligand) or HH signaling (Figure 7I) in the papilla epithelium could not reconstitute TB, and thus maintained HHIP expression in the papilla apex (Figure 7F). Overall, these data demonstrate a correlation between ectopic HHIP expression in FP following HPI, and an inability of those papillae to recover following the cessation of HPI.

***Hhip* is ectopically expressed after chorda tympani/lingual nerve cut**

The TB in anterior tongue FP are innervated by the chorda tympani (CT) nerve, which is also a source of SHH ligand, along with the TB.^{1,4,7} However, the retained innervation after HPI with sonidegib, *cSmoKO*, *cGli2KO* or *cGli2 C4* is not sufficient to maintain TB, or to initiate TB regeneration when there is HH signaling disruption in the epithelium.^{2–5} TB integrity depends both on intact HH signaling in the lingual epithelium and on intact nerves.⁹ Whereas TB are innervated by the CT only, with soma in the geniculate ganglion (GG), the FP and FILIF basal epithelial cells are innervated by the lingual (LN) nerve, with soma in the trigeminal ganglion (TG).⁹ The LN and CT travel into the tongue and base of the FP together, and then segregate their distributions within the FP. To test the effects of elimination of neural support on *Hhip* expression, we studied the distribution of *Hhip* and HHIP after unilateral denervation of CT/LN nerves. The contralateral tongue, with no nerve cut, served as a Control.

In serial tongue sections, at 21 days after combined CT/LN nerve cut we categorized FP into three FP/TB types (I, II, III) and evaluated TB presence by immunostaining with the TB cell marker, K8 (Figure 8A–F). Innervation was assessed with antibodies to P2X3 (CT nerves, Figure A–C) and NF (LN and CT nerves, Figure 8D–F). Tissues in the tongue half with nerve cut were compared to those in the Control side of the tongue, where CT/LN nerves were exposed but not cut. In Control tongue more than 80% of FP are Typical Type I and these have robust innervation from the CT and LN nerves (Figure 8A,D; Figure 8J). As expected, in this control tissue, *Hhip* expression and HHIP localization are restricted to FILIF (Figure 8D',G).

However, at 21 days after nerve cut, 80% of FP are either Type II or Type III (Figure 8J) and in these FP the CT/LN nerves are either much reduced or eliminated (Figure 8B,C,E,F). In the half tongue after unilateral nerve cut we observed ectopic expression of both *Hhip* (Figure 8E',F') and HHIP (Figure H,I) at the FP apex, with or without TB remnants, in addition to the retained expression in the FILIF. The percentages of FP with ectopic *Hhip* (Figure 8K) and HHIP (Figure 8L) were significantly increased after CT/LN nerve cut compared to Control. These data demonstrate that CT/LN nerve cut mimics the phenotype observed with either pharmacologic or genetic HH pathway blockade. The pattern of ectopic *Hhip* gene or protein expression in altered FP/TB after nerve cut is similar to pharmacologic or genetic HH pathway disruption (cf. Figures 6–7). However, with sonidegib treatment or in genetic deletion/repression models, there was a reduction or elimination of only the TB source of SHH.^{2–5} In contrast, after CT/LN nerve cut, there is reduced epithelial SHH associated with loss of TB, reduced neural SHH associated with elimination of nerves in Atypical FP/TB,²⁶ and, there is no retained TB source or neural source of SHH in Atypical FP/No TB (Figure 9A,B). Thus, ectopic *Hhip* expression in altered FP seems to be maintained independently of the presence of SHH. In addition to deprivation of SHH ligand in the nerve cut model, other taste nerve-derived growth factors are also lost. However, these factors are unlikely to contribute to HHIP expression as ectopic HHIP is still observed in FP apex in HPI models where innervation is retained (Figures 6–7).

Ectopic HHIP correlates with reduced HH signaling after CT/LN cut

To better understand the induction of ectopic *Hhip* following CT/LN cut, we assessed HHIP in association with *Gli1^{lacZ}* expression to read out HH pathway activity (Figure 10A–A''). CT/LN nerve cut resulted in reduced K8+ TB cells and *Gli1^{lacZ}*₊ cells from the epithelium of Atypical FP/TB, Type II (Figure 10B–D,B''–D''). There were no K8+ TB cells or *Gli1^{lacZ}*₊ cells in the epithelium of Atypical FP/No TB, Type III (Figure 10E,E'').

In Atypical FP/TB (Type II) with epithelial *Gli1^{lacZ}*₊ expression in the FP walls, there was no ectopic HHIP labeling (Figure 10B'). However, with the loss of *Gli1^{lacZ}*₊ cells from one wall of the FP basal epithelium, there was a simultaneous induction of HHIP on that side only of the FP apex (Figure 10C'). In addition, when *Gli1^{lacZ}*₊ cells were completely lost from both walls of the Atypical FP/TB, ectopic HHIP expression was induced on both the sides of the TB remnant, bracketing the remaining K8+ TB cells (Figure 10D', **arrows**). Finally, the elimination of epithelial *Gli1^{lacZ}* expression in Atypical FP/No TB (Type III) was associated with sustained expression of HHIP in the FILIF and robust ectopic

expression at the location of the former TB (Figure 10E'). These data demonstrate that ectopic HHIP correlates with loss of HH signaling in the FP.

Ectopic *Ptch1* expression in FP during HH pathway inhibition

Given that *Ptch1* overlaps with HHIP in FILIF (Figure 5G''), we investigated the consequences of HH pathway inhibition on *Ptch1* expression. In Vehicle-treated tongues, *Ptch1^{lacZ}* cells were present in FP (basal, perigemmal and stromal cells) and FILIF (subset of cells; Figure 11A,A''). After sonidegib treatment to inhibit the HH pathway, in Atypical FP/TB, *Ptch1^{lacZ}* expression was lost from FP basal walls and perigemmal cells (Figure 11B–D), similar to *Gli1^{lacZ}*.^{3,4} On the other hand, gene expression was maintained in FILIF, and in the FP apex at a location close to ectopic *Hhip* gene and protein expression (Figure 11B–D, cf. Figure 6,8,10). We used HHIP immunostaining (Figure 11A'–D') to confirm that *Ptch1* and HHIP expression overlap at the apex of Atypical FP/No TB (Type III) along with the usual co-expression in FILIF (Figure 11A'–D'', yellow dotted lines). These data indicate that *Ptch1* is expressed in a HH-dependent manner in FP (like *Gli1*), but in a HH-independent manner in FILIF (like *Hhip*). Further, our data indicate that both ectopic *Ptch1* (Figure 11E) and *Hhip* (cf. Figure 8K) are induced in Atypical FP with or without TB (Type II and III) during HPI.

Overall the results suggest that, unlike other HH-dependent tissues, there are distinct expression patterns of *Ptch1*, *Gli1* and *Hhip* in the adult tongue. Specifically, we find that *Ptch1* and *Hhip* are expressed in a HH-independent manner in FILIF, and propose that this expression may restrict SHH signaling in these nongustatory taste organs. Further functional experiments will be required to define the FILIF-specific contribution of these key HH pathway antagonists to taste organ homeostasis.

Discussion

We have investigated a potential contribution of HH pathway antagonists to adult tongue homeostasis. Remarkably, we find that HHIP expression is restricted to FILIF during normal taste organ homeostasis. This contrasts with the known expression of the general HH pathway target *Gli1*,³ and suggests that *Hhip* is not a direct transcriptional target in either HH-responsive epithelial cells of the FP, or in the HH-responsive stroma that underlies this epithelium. Further, we find that pharmacologic inhibition of HH signaling, genetic abrogation of HH pathway activity (using three different genetic models), and physical ablation of nerve-derived HH ligands (through nerve cut experiments), all result in ectopic *Hhip* expression in altered FP. These data suggest that *Hhip* expression in the FP is repressed by active HH signaling, and that there is HH-independent regulation of *Hhip* expression in FILIF. Notably, *Ptch1* is similarly expressed in FILIF, and, like *Hhip*, is ectopically expressed during HPI. These results suggest a model where HH pathway antagonists are expressed in a HH-independent fashion in FILIF to limit the range of HH signaling, and that their ectopic expression following HPI acts to regulate a cellular transformation of FP to FILIF-like.

HHIP is a secreted HH pathway antagonist.^{13,16} However, it differentially localizes to the cell surface and within the extracellular matrix depending on interactions with heparan

sulfate proteoglycans (HSPGs).¹³ Using a combination of a *Hhip^{lacZ}* reporter and HHIP antibody, we demonstrate that HHIP remains closely associated with the cells that produce this HH pathway antagonist. These data suggest that the cell surface-associated HSPGs synthesized by these cells contain the appropriate sulfation patterns necessary to bind and retain HHIP in close proximity to its site of production. That these cells also express *Ptch1* indicates a level of redundancy to prevent inappropriate activation of HH signaling in the FILIF. Given that *Ptch1* and *Hhip* are simultaneously expressed in these cells in a HH-independent fashion, future experiments examining GLI-independent inputs into their expression will yield important insights into the transcriptional regulation of their expression in FILIF.

HH pathway inhibition pharmacologically, genetically or with nerve cut results in ectopic *Hhip* expression in the FP apex where TB had been located, in addition to a sustained expression in the FILIF. Notably, ectopic *Hhip* is not detected in the underlying stroma during HPI; this suggests either that there are epithelial-specific inputs to *Hhip* gene expression, or that additional, stromal-specific inputs continue to repress *Hhip* despite the loss of HH pathway activity.

Although there is known *Hhip* expression in other tissues^{12,27} this is the first detailed demonstration in the tongue. Strikingly, the lingual expression pattern of *Hhip* is in the nongustatory FILIF papillae only, in contrast to expression of HH signaling elements, *Gli1*, *Gli2* and *Ptch1*, in FP, CV and FOL taste papillae.

Cell type-specific regulation of HH pathway components in the adult tongue

We have identified distinct *Gli* expression in tongue epithelium: *Gli1* is expressed in basal and perigemmal cells of the FP, but sharply ends at the base of the FP epithelium, before the start of the inter-FP region, creating a distinct border for FP epithelium. In contrast, *Gli2* is expressed throughout basal cells of the tongue including FP and FILIF (Figure 4C,C'). Therefore, transcriptional targets of these two key effectors of HH signaling might overlap in FP, but presumably are different in FILIF. We have shown that *Gli1* expression is dependent on *Gli2* and that *Gli1* deletion did not disrupt FP/TB² suggesting that GLI2 is primarily a transcriptional activator while *Gli1* is a target gene of the HH pathway in tongue. As *Gli2* deletion and suppression did not alter HHIP expression in FILIF, and elimination of *Gli1* is required for ectopic HHIP expression in FP, it is likely that *Hhip* is not a transcriptional target of either GLI1 or GLI2 in the tongue.

Our data also demonstrate that *Ptch1* and *Gli1* are expressed in distinct domains in the adult tongue. That is, whereas both *Ptch1* and *Gli1* are expressed in a HH-responsive fashion in epithelial cells near the TB in FP, and in stromal cells underlying this epithelium, *Ptch1* is additionally expressed in the FILIF epithelium. Importantly, this FILIF expression is HH-independent (i.e., it is maintained after pharmacologic HH pathway blockade), suggesting a separate transcriptional input for FILIF-specific *Ptch1* expression in the adult tongue. These data highlight the need to better understand the transcriptional regulation of HH targets in adult lingual organs, including the differences in epithelial and stromal activation of HH targets, as well as HH-dependent induction of *Gli1* and *Ptch1* in FP, and HH-independent induction of *Ptch1* and *Hhip* in FILIF.

FILIF and restricted HH antagonist expression

FILIF are unique in coincident expression of both *Hhip* and *Ptch1*. These non-gustatory organs, without TB and without HH ligand in the epithelium, are the most numerous of the four main types of lingual papillae (FP, CV, FOL, FILIF). FILIF function in bolus manipulation and other oral sensory functions.^{25,28} Most studies on homeostatic regulation of lingual organs that have focused on the taste papillae and included investigations of FILIF are mainly during embryonic/developmental stages.^{29–31} The basal epithelial cells of each FILIF differentiate to oriented tapering columns with discrete boundaries for anterior and posterior suprabasal layers.²³ Although several keratins and transcription factors are expressed in FILIF,^{25,31,32} they are not limited to the FILIF papillae *per se* but rather are throughout the entire lingual epithelium or only the buttress columns between FILIF.^{24,33} The anterior cell column differs from the posterior in having keratohyalin granules in granular cell layers and ‘soft’ keratins^{23,24} that provide structural flexibility and tissue-specific functions.³⁴ Within the FILIF we have demonstrated that *Hhip* gene and protein, and *Ptch1* expressions are restricted in a specific set of cells of the anterior papilla face only.

HH signaling, inhibition and HHIP expression

Conspicuously, the nongustatory FILIF are the only lingual papillae where there is no HH ligand in the epithelium and where HH signaling is inactive, and they are the sole locations for HHIP expression. This is intriguing because HH signaling is reported to regulate *Hhip* transcription of HHIP.^{12,18,35} Within the gustatory FP, SHH ligand is within TB cells and signals via paracrine signaling to perigemmal cells and cells of the FP basal epithelial compartment.⁶ However, TB cells are not present in FILIF papillae and thus there is no resident epithelial ligand to drive HH signaling in these papillae. On the other hand, SHH ligand is also expressed in lingual nerves and ganglia (TG and GG).^{1,4,7} The LN nerve, with soma in the TG, innervates FILIF and could possibly be a source of HH ligand.⁹

To address interactions between HH signaling and HHIP expression, we used various models including pharmacologic SMO inhibition, genetic deletion of *Smo* and *Gli2*, expression of a *Gli2* repressor, and severing the CT/LN nerve. These approaches suppressed HH signaling, eliminated TB and therefore SHH ligand in FP epithelium, and with nerve cut experiments eliminated TB and innervation and thus two sources of SHH. In all of the inhibition models the specific HHIP expression pattern was retained in FILIF. Thus, although *Hhip* is a transcriptional target of HH signaling, inhibition of pathway activity via *Smo* inhibition/deletion and *Gli2* deletion/suppression or elimination of SHH ligand by CT/LN nerve cut does not affect its expression in FILIF. Overall our data indicate HH pathway component-independent expression of HHIP in FILIF.

Strikingly, in all of the models of HH signaling inhibition there was ectopic HHIP expression at the FP apex. Our data with short term *Smo* deletion indicated that the absence of HH pathway activity alone did not induce ectopic HHIP, as observed in Typical FP/TB after whole body *Smo* deletion for 5 days. However, HHIP emerged in Atypical FP without TB or TB remnants simultaneously with loss of *Gli1^{lacZ}* from the FP epithelium. Similarly in our recovery studies where HH signaling inhibition is discontinued, HHIP was only in Atypical FPs and not in recovered Typical FP/TB. Typical TB express SHH which is

reduced or eliminated in Atypical FPs after HH signaling inhibition.^{2–5} Our data suggest a required reduction/elimination of SHH ligand and *Gli1*+ HH-responding cells for ectopic HHIP expression in lingual FP. HHIP is reported to have an inverse relationship with SHH and *Gli1* expression during angiogenesis also.³⁶ Absence of SHH in Atypical FP/No TB in parallel with ectopic HHIP reinforces the idea that maintenance of HHIP expression in FILIF does not require SHH ligand. Previous *in vitro* studies also indicated that HHIP maintenance is independent of interaction between SHH and HHIP.¹⁶

Proposals for HH signaling and HHIP interactions

Our study reveals dynamic changes in *Hhip* and *Ptch1* expression during HH pathway inhibition in the adult tongue. Based on these data, we propose the following model— in control tissue, FP are HH-dependent structures with SHH in TB basal cells, and *Gli1* in epithelial and perigemmal cells (Figure 12A). In contrast, FILIF are HH-independent organs that express HH pathway antagonists. When HH pathway inhibition results in a partial elimination of *Gli1*+ cells in Atypical FP/TB, corresponding ectopic HHIP was only in cells that lack *Gli1* (Figure 12B). Once *Gli1*+ cells are eliminated from both sides of FP walls with complete loss of SHH, the entire FP apex gained HHIP expression and acquired FILIF-like conical morphology (Figure 12C). Given that HHIP is observed in FILIF where SHH and *Gli1*+ HH-responding cells are not expressed we propose that HHIP might inhibit HH signaling in FILIF by antagonizing SHH and downstream *Gli1*+ HH-responding cells (Figure 12D). On the contrary, in FP the HH pathway activity as illustrated by *Gli1*+ cells inhibits HHIP expression. Moreover, it seems that intact SHH also attenuates HHIP directly or indirectly by activating *Gli1*+ cells (Figure 12E).

Secreted SHH ligand acts via paracrine signaling to *Gli1^{lacZ}*+ cells in the perigemmal TB region and in the basal epithelial cells of the FP walls (Figure 12E).^{6,8} Notably, beyond the FP epithelial walls there is no *Gli1*+ expression. Thus, we also propose that the secreted antagonist HHIP signals through the FILIF basal epithelial cells to the basal-most epithelial point of the rete peg, at the juncture where FP and FILIF morphologies meet. In the FP basal epithelial cells, secreted SHH could internalize and degrade HHIP as reported *in vitro*,¹⁶ thus limiting our ability to visualize this population of HHIP. HHIP-mediated sequestration of SHH would prevent further signaling (Figure 12E). Redundant HH pathway antagonism by PTCH1 would further block HH signaling, resulting in the formation of a FILIF structure. Importantly, there is precedent for HH pathway inhibition in the formation of other structures, specifically the developing pancreas, where combined HHIP and PTCH1 function also play a key role.^{37,38} Work from Castillo et al³⁹ driving SHH expression in K14+ lingual epithelium and from Lu et al⁷ using systemic treatment with the HH agonist, SAG both result in the formation of ectopic TB-like structures in non-taste FILIF. It is important to note that these ‘ectopic TB’ are K8+ cell clusters with no nerve fibers or a taste pore. These data raise the question of whether ectopic SHH signaling leads to disruption of FILIF differentiation or transformation of FILIF to FP. It is possible that HHIP functions not to protect FILIF but to regulate TB numbers. To distinguish between these possibilities, FILIF-specific conditional deletion of *Ptch1* and/or *Hhip* (and possibly *Ptch2*)¹⁴ will be necessary.

Experimental Procedures

Animals

All animal use and care procedures followed guidelines of the National Institutes of Health and approved protocols of the University of Michigan Institutional Animal Care and Use Committee. Male and female mice, aged 8 to 12 weeks, were used.

Mouse models/strains

lacZ reporters: Mice carrying lacZ alleles for the target gene/HH responding Gli1 (*Gli1^{lacZ/+}*), transcriptional activator, Gli2 (*Gli2^{lacZ/+}*); HH-receptor Ptch1 (*Ptch1^{lacZ/+}*), and HH antagonist Hhip (*Hhip^{lacZ/+}*) were maintained on mixed (C57BL/6J and 129S4/SvJaeJ) backgrounds. For each reporter, observations were made in at least 3 mice.

HH pathway inhibition (HPI): SMO inhibition with Sonidegib: C57BL/6J mice were treated with 20mg/kg sonidegib (ChemieTek, CT-LDE225) prepared in vehicle containing PEG400/ 5% dextrose (Sigma-Aldrich) in H₂O (75:25 v/v) or Vehicle alone for 16 days by daily oral gavage to pharmacologically inhibit SMO.^{3,4} For Recovery experiments, sonidegib treatment was discontinued after 16 days and animals were maintained on standard diet for 14 days.⁴

epi-*Smo* deletion, *cSmoKO*: Mice for doxycycline-dependent, Cre-driven deletion of *Smo* (*K5-rtTA;tetO-Cre;Smo^{fl/fl}*) from K5+ basal epithelium were studied after 15 – 24 days. *SmoKO*, *Smo* whole body deletion (*R26^{M2rtTA/+};tetO-Cre;Smo^{fl/fl}*)⁴ for 5 days was used for short term HPI.

epi-*Gli2* deletion, *cGli2KO*: Mice for doxycycline-dependent, Cre-driven deletion of *Gli2* (*K5-rtTA;tetO-Cre;Gli2^{fl/fl}*) in K5-expressing basal cells² were studied after 35 days.

epi-*Gli2* suppression, *cGli2 C4*: Mice for doxycycline-dependent, dominant-negative repression of GLI targets in K5-expressing, basal epithelial cells (*K5-rtTA;tetO-Gli2 C4*)² were investigated after 28 days.

Littermates negative for *K5-rtTA* and/or *tetO-Cre* were used as controls for genetic HPI models.

K5-rtTA mice were obtained from Adam Glick (Pennsylvania State University). These strains were obtained from The Jackson Laboratory: *Gli1^{lacZ/+}* (Stock No: 008211); *Gli2^{lacZ/+}* (Stock No: 007922); *Ptch1^{lacZ/+}* (Stock no: 00308); *Hhip^{lacZ/+}* (Stock No: 006241); *Smo^{fl/fl}* or *Smo^{tm2Amc/J}* (Stock No: 004526); *Gli2^{fl/fl}* (Stock No: 007926); *tetO-Cre* (Stock No: 006224); *R26^{M2rtTA/+}* or *B6.Cg-Gt(ROSA)26Sor^{tm1(rtTA*M2)Jae/J}* (Stock No: 006965). *tetO-Gli2 C4* mice were generated using a mouse *Gli2 C4* cDNA.² Doxycycline was given in chow at 6g doxycycline/kg chow (Bio-Serv), continuously throughout the treatment period. For each mouse model, 1–2 tongues were analyzed per Control and Experimental group. From 8 to 30 fungiform papillae per tongue were analyzed.

Nerve cut experiments

Gli1^{LacZ/+}, *Gli2^{LacZ/+}* and *Hhip^{LacZ/+}* reporter mice were used for nerve cut studies. The chorda tympani (CT) and lingual (LN) nerves are approached via a ventral incision in the neck, with the anesthetized mouse in a supine position.²⁶ Unilateral denervation of the combined CT and LN nerve was made using aseptic conditions. A few mm of the CT/LN nerve, where it runs deep in the neck, were removed to permanently interrupt the nerves. On the uncut, contralateral Control side, the nerves were fully exposed and the neck incision then closed without further disturbance. Animals were maintained on a water-circulating heating pad until fully awake and moving comfortably. Analgesic injections were used for 24–48 hours post-surgery. Tongue tissues were analyzed 21 days after the CT/LN nerve cut. Observations were made in at least 3 experimental and 3 control mice. Actual animal numbers analyzed are included in the graphs.

Tissue analyses

Tongues were collected from adult mice and at specified time points for HPI models and nerve cut studies, and prepared for tissue analysis.

Tissue Dissection, Processing: Mice were euthanized with CO₂ overdose. Tongues on mandibles and soft palates were dissected and fixed at 4°C in 4% PFA in PBS and processed for histology, immunostaining, or X-gal staining as described previously.^{2–5} Fixed tongues were dissected into the anterior tongue, distal to the intermolar eminence, and a posterior tongue piece that included the CV and FOL papillae. The anterior tongue piece was then bisected down the midline, or median furrow, to yield two half pieces.

Histology: The anterior half tongue, the CV/foliate, and the soft palate were fixed overnight for paraffin embedding, serial sectioning at 6 µm, in sagittal plane (anterior half, FP) or horizontal plane (posterior CV/FOL), or at 10 µm in coronal plane (soft palate) and staining with H&E for morphological analysis.

Immunostaining: The anterior half tongue, the CV/FOL and the soft palate were fixed for 2h–5h, cryoprotected with 30% sucrose in PBS and embedded in O.C.T. Serial sagittal sections (FP), horizontal sections (CV/FOL), or coronal sections (soft palate) were cut at 10 µm.^{2–5} Immunoreactions were performed as described.^{2–5} Primary antibodies were used to identify HH-antagonist HHIP (1:5000, developed in Allen lab¹⁴; 1:500, AF1568, R&D Systems), TB cells (K8, 1:1000 TROMA1, DSHB), HH ligand (SHH, 0.1 µg/ml, AF464, R&D Systems), and nerves (Neurofilament-H, NF 1:1000, NB300–135, Novus Biologicals; P2X3, 1:2000, NB100–1654, Novus Biologicals). Secondary antibodies were Alexa Fluor conjugates 488 or 568 (Life Science Technologies, 1:500). Sections were mounted with Vectashield mounting medium containing DAPI.

X-Gal staining: Tongues were fixed for 2h. For whole tongue X-Gal staining, tissues were incubated in X-Gal solution for 18–72h at 37°C, washed with PBS and imaged. For tongue sections, tissues were cryoprotected and processed as described for immunostaining. *LacZ* reporter activity was visualized by incubating tongue sections in X-Gal solution for

18h–48h. X-gal staining of sections was followed by immunostaining of TB cells (K8), HH-antagonist (HHIP) or innervation (NF).

Hhip gene and protein expression analyses: Sectioned FP, CV or FOL taste papillae, and the soft palate were evaluated for the presence or absence of X-Gal expression for *Hhip^{lacZ}* or HHIP immunostaining.

Imaging

Whole tongues were imaged with a Leica M165FC stereomicroscope and CellSens software. Tissue section images were acquired with a Nikon Eclipse 80i microscope and Nikon DS Ri2 camera system and NIS software. Adjustments were made for brightness and contrast in parallel across photomicrographs in one Figure. Figure panels were assembled with Adobe Photoshop.

Data analysis for nerve cut experiment

Quantification of fungiform papillae (FP) and taste buds (TB): K8+ TB cell immunostaining was used to define three different FP/TB categories: (I) Typical FP/TB, (II) Atypical FP/TB and (III) Atypical FP/No TB. These categories are illustrated in Figs 5–7 and explained in Results.

We studied 6 tongues at 21 day after CT/LN nerve cut or Control group. Data are reported as percentage of FP/TB Type I, II or III, in a half tongue.

Quantitation of *Hhip^{lacZ/+}* gene and HHIP protein expression: We quantified presence of *Hhip* expression after X-Gal staining of *Hhip^{lacZ/+}* tongue tissues in CT/LN nerve cut and contralateral Control group. Three tongues were analyzed per treatment group. Fungiform papillae in complete serial sections were studied for *lacZ+* cells and counted. Data are reported as percentage of FP positive for *Hhip^{lacZ/+}* cells in the entire half tongue.

We used antibodies to HHIP to label HH-antagonist cells in FP. Two *Gli1^{lacZ/+}* and one *Gli2^{lacZ/+}* mice at 21 days after CT/LN nerve cut were examined. Complete half tongues, Control and Cut side, were screened for HHIP+ cells. FP, with any cells of the serial section positive for HHIP were counted and the data are presented as percentage of FP expressing HHIP. Average number of FP counted for each half tongue was 27.

Data analysis for sonidegib experiment in *Ptch1^{lacZ}* mice—Quantitation of *Ptch1^{lacZ/+}* expression: X-Gal staining of *Ptch1^{lacZ/+}* reporter tongue reveals expression in FP basal, perigemmal and stromal cells and was categorized as Typical expression (Figure 11A). After HPI with sonidegib, ectopic and some remaining *lacZ* expression was observed in FP and categorized as Ectopic expression (Figure 11B–D). Fungiform papillae in complete serial sections were studied for quantitation. We counted Typical and Ectopic *Ptch1* expression after X-Gal staining of *Ptch1^{lacZ/+}* tongue tissues in Vehicle and Sonidegib treated groups. Numbers of tongues analyzed are included in the graph for Fig 8. Data are reported as percentage of FP having Typical or Ectopic *Ptch1^{lacZ/+}* expression. An average of 20 FP were counted per tongue.

Statistics: For analysis of FP/TB count, *Hhip*^{lacZ/+} and HHIP expression between two groups (Control and CT/LN nerve cut), and Typical and Ectopic *Ptch1* expression we used the independent sample t-test to compare differences between treatments. Actual numbers of mice/tongues examined for statistical analyses are included in graphs. Data in Figures are presented as mean ± SEM. Significance levels of *p<0.001 and **p<0.05 were used.

Acknowledgments

We thank members of the Allen and Dlugosz laboratories for ongoing discussions about the research.

Grant Sponsor and Grant Number: National Institutes of Health (NIH) National Institute on Deafness and Other Communication Disorders (NIDCD)

NIH NIDCD Multi PI R01 DC0114428

NIH NIDCD ECR R21 1R21DC017799

Funding statement: This research was funded by NIH National Institute on Deafness and Other Communication Disorders (NIDCD) NIH NIDCD Multi PI R01 DC0114428 to BLA, AAD, CMM; and, NIH NIDCD ECR R21 1R21DC017799 to AK.

The funders had no role in the design of the study; in the collection, analyses, or interpretation of data; in the writing of the manuscript, or in the decision to publish the results.

References

1. Castillo-Azofeifa D, Losacco JT, Salcedo E, Golden EJ, Finger TE, Barlow LA. Sonic hedgehog from both nerves and epithelium is a key trophic factor for taste bud maintenance. *Development*. Sep 1 2017;144(17):3054–3065. 10.1242/dev.150342. [PubMed: 28743797]
2. Ermilov AN, Kumari A, Li L, et al. Maintenance of taste organs is strictly dependent on epithelial Hedgehog/GLI signaling. *PLoS genetics*. Nov 2016;12(11):e1006442. 10.1371/journal.pgen.1006442.
3. Kumari A, Ermilov AN, Allen BL, Bradley RM, Dlugosz AA, Mistretta CM. Hedgehog pathway blockade with the cancer drug LDE225 disrupts taste organs and taste sensation. *J Neurophysiol*. Feb 1 2015;113(3):1034–40. 10.1152/jn.00822.2014. [PubMed: 25392175]
4. Kumari A, Ermilov AN, Grachtchouk M, et al. Recovery of taste organs and sensory function after severe loss from Hedgehog/Smoothed inhibition with cancer drug sonidegib. *Proc Natl Acad Sci U S A*. Nov 28 2017;114(48):E10369-E10378. 10.1073/pnas.1712881114.
5. Kumari A, Yokota Y, Li L, Bradley RM, Mistretta CM. Species generalization and differences in Hedgehog pathway regulation of fungiform and circumvallate papilla taste function and somatosensation demonstrated with sonidegib. *Sci Rep*. 2018/11/01 2018;8(1):16150. 10.1038/s41598-018-34399-3. [PubMed: 30385780]
6. Liu HX, Ermilov A, Grachtchouk M, et al. Multiple Shh signaling centers participate in fungiform papilla and taste bud formation and maintenance. *Developmental biology*. Oct 1 2013;382(1):82–97. 10.1016/j.ydbio.2013.07.022. [PubMed: 23916850]
7. Lu WJ, Mann RK, Nguyen A, et al. Neuronal delivery of Hedgehog directs spatial patterning of taste organ regeneration. *Proc Natl Acad Sci U S A*. Jan 9 2018;115(2):E200–E209. 10.1073/pnas.1719109115. [PubMed: 29279401]
8. Mistretta CM, Kumari A. Tongue and Taste Organ Biology and Function: Homeostasis Maintained by Hedgehog Signaling. *Annu Rev Physiol*. 2017;79 24.1–22. 10.1146/annurev-physiol-022516-034202
9. Mistretta CM, Kumari A. Hedgehog Signaling Regulates Taste Organs and Oral Sensation: Distinctive Roles in the Epithelium, Stroma, and Innervation. *Int J Mol Sci*. Mar 16 2019;20(6). 10.3390/ijms20061341.

10. Briscoe J, Therond PP. The mechanisms of Hedgehog signalling and its roles in development and disease. *Nat Rev Mol Cell Biol.* Jul 2013;14(7):416–29. 10.1038/nrm3598. [PubMed: 23719536]
11. Chuang PT, Kawcak T, McMahon AP. Feedback control of mammalian Hedgehog signaling by the Hedgehog-binding protein, Hip1, modulates Fgf signaling during branching morphogenesis of the lung. *Genes Dev.* Feb 1 2003;17(3):342–7. 10.1101/gad.1026303. [PubMed: 12569124]
12. Chuang PT, McMahon AP. Vertebrate Hedgehog signalling modulated by induction of a Hedgehog-binding protein. *Nature.* Feb 18 1999;397(6720):617–21. 10.1038/17611. [PubMed: 10050855]
13. Holtz AM, Griffiths SC, Davis SJ, Bishop B, Siebold C, Allen BL. Secreted HHIP1 interacts with heparan sulfate and regulates Hedgehog ligand localization and function. *J Cell Biol.* Jun 8 2015;209(5):739–57. 10.1083/jcb.201411024. [PubMed: 26056142]
14. Holtz AM, Peterson KA, Nishi Y, et al. Essential role for ligand-dependent feedback antagonism of vertebrate hedgehog signaling by PTCH1, PTCH2 and HHIP1 during neural patterning. *Development.* Aug 2013;140(16):3423–34. 10.1242/dev.095083. [PubMed: 23900540]
15. Jeong J, McMahon AP. Growth and pattern of the mammalian neural tube are governed by partially overlapping feedback activities of the hedgehog antagonists patched 1 and Hhip1. *Development.* Jan 2005;132(1):143–54. 10.1242/dev.01566. [PubMed: 15576403]
16. Kwong L, Bijlsma MF, Roelink H. Shh-mediated degradation of Hhip allows cell autonomous and non-cell autonomous Shh signalling. *Nat Commun.* Sep 12 2014;5:4849. 10.1038/ncomms5849. [PubMed: 25215859]
17. Peterson KA, Nishi Y, Ma W, et al. Neural-specific Sox2 input and differential Gli-binding affinity provide context and positional information in Shh-directed neural patterning. *Genes Dev.* Dec 15 2012;26(24):2802–16. 10.1101/gad.207142.112. [PubMed: 23249739]
18. Vokes SA, Ji H, McCuine S, et al. Genomic characterization of Gli-activator targets in sonic hedgehog-mediated neural patterning. *Development.* May 2007;134(10):1977–89. 10.1242/dev.001966. [PubMed: 17442700]
19. Vokes SA, Ji H, Wong WH, McMahon AP. A genome-scale analysis of the cis-regulatory circuitry underlying sonic hedgehog-mediated patterning of the mammalian limb. *Genes Dev.* Oct 1 2008;22(19):2651–63. 10.1101/gad.1693008. [PubMed: 18832070]
20. Lao T, Jiang Z, Yun J, et al. Hhip haploinsufficiency sensitizes mice to age-related emphysema. *Proc Natl Acad Sci U S A.* Aug 9 2016;113(32):E4681–7. 10.1073/pnas.1602342113. [PubMed: 27444019]
21. Cleaton-Jones P. Histological observations in the soft palate of the albino rat. *Journal of anatomy.* 1971;110(Pt 1):39–47. [PubMed: 5140515]
22. Miller IJ, Spangler K. Taste bud distribution and innervation on the palate of rat. 1982:99–108. 10.1093/chemse/7.1.99
23. Hume WJ, Potten CS. The ordered columnar structure of mouse filiform papillae. *J Cell Sci.* Oct 1976;22(1):149–60. 10.1093/chemse/7.1.99 [PubMed: 977666]
24. Iwasaki S, Okumura Y, Kumakura M. Ultrastructural study of the relationship between the morphogenesis of filiform papillae and the keratinization of the lingual epithelium in the mouse. *Cells Tissues Organs.* 1999;165(2):91–103. 10.1159/000016679. [PubMed: 10516422]
25. Wong P, Colucci-Guyon E, Takahashi K, Gu C, Babinet C, Coulombe PA. Introducing a null mutation in the mouse K6alpha and K6beta genes reveals their essential structural role in the oral mucosa. *J Cell Biol.* Aug 21 2000;150(4):921–8. 10.1083/jcb.150.4.921. [PubMed: 10953016]
26. Kumari A, Allen BL, Bradley RM, Dlugosz AA, Mistretta CM. Role of innervation in HH signaling in the adult mouse fungiform taste papilla. Program no. 50.27 / W4. Paper presented at: Neuroscience Abstracts; 2016; San Diego, CA. <https://www.abstractsonline.com/pp8/index.html#!/4071/presentation/8805>
27. Olsen CL, Hsu PP, Glienke J, Rubanyi GM, Brooks AR. Hedgehog-interacting protein is highly expressed in endothelial cells but down-regulated during angiogenesis and in several human tumors. *BMC Cancer.* Aug 4 2004;4:43. 10.1186/1471-2407-4-43. [PubMed: 15294024]
28. Moayed Y, Duenas-Bianchi LF, Lumpkin EA. Somatosensory innervation of the oral mucosa of adult and aging mice. *Sci Rep.* Jul 2 2018;8(1):9975. 10.1038/s41598-018-28195-2. [PubMed: 29967482]

29. Byrd KM, Lough KJ, Patel JH, Descovich CP, Curtis TA, Williams SE. LGN plays distinct roles in oral epithelial stratification, filiform papilla morphogenesis and hair follicle development. *Development*. Aug 1 2016;143(15):2803–17. 10.1242/dev.136010. [PubMed: 27317810]
30. Jonker L, Kist R, Aw A, Wappler I, Peters H. Pax9 is required for filiform papilla development and suppresses skin-specific differentiation of the mammalian tongue epithelium. *Mech Dev*. Nov 2004;121(11):1313–22. 10.1016/j.mod.2004.07.002. [PubMed: 15454262]
31. Nishiguchi Y, Ohmoto M, Koki J, et al. Bcl11b/Ctip2 is required for development of lingual papillae in mice. *Developmental biology*. Aug 1 2016;416(1):98–110. 10.1016/j.ydbio.2016.06.001. [PubMed: 27287879]
32. Kawasaki M, Kawasaki K, Oommen S, et al. Regional regulation of Filiform tongue papillae development by Ikkalpha/Irf6. *Dev Dyn*. Sep 2016;245(9):937–46. 10.1002/dvdy.24427. [PubMed: 27302476]
33. Tanaka T, Komai Y, Tokuyama Y, et al. Identification of stem cells that maintain and regenerate lingual keratinized epithelial cells. *Nat Cell Biol*. May 2013;15(5):511–8. 10.1038/ncb2719. [PubMed: 23563490]
34. Coulombe PA, Omary MB. ‘Hard’ and ‘soft’ principles defining the structure, function and regulation of keratin intermediate filaments. *Curr Opin Cell Biol*. Feb 2002;14(1):110–22. 10.1016/s0955-0674(01)00301-5. [PubMed: 11792552]
35. Katoh Y, Katoh M. Hedgehog target genes: mechanisms of carcinogenesis induced by aberrant hedgehog signaling activation. *Curr Mol Med*. Sep 2009;9(7):873–86. 10.2174/156652409789105570. [PubMed: 19860666]
36. Lee BNR, Son YS, Lee D, et al. Hedgehog-Interacting Protein (HIP) Regulates Apoptosis Evasion and Angiogenic Function of Late Endothelial Progenitor Cells. *Sci Rep*. Sep 29 2017;7(1):12449. 10.1038/s41598-017-12571-5. [PubMed: 28963460]
37. Hebrok M, Kim SK, Melton DA. Notochord repression of endodermal Sonic hedgehog permits pancreas development. *Genes Dev*. Jun 1 1998;12(11):1705–13. 10.1101/gad.12.11.1705. [PubMed: 9620856]
38. Kawahira H, Ma NH, Tzanakakis ES, McMahon AP, Chuang PT, Hebrok M. Combined activities of hedgehog signaling inhibitors regulate pancreas development. *Development*. Oct 2003;130(20):4871–9. 10.1242/dev.00653. [PubMed: 12917290]
39. Castillo D, Seidel K, Salcedo E, et al. Induction of ectopic taste buds by SHH reveals the competency and plasticity of adult lingual epithelium. *Development*. Aug 2014;141(15):2993–3002. 10.1242/dev.107631. [PubMed: 24993944]

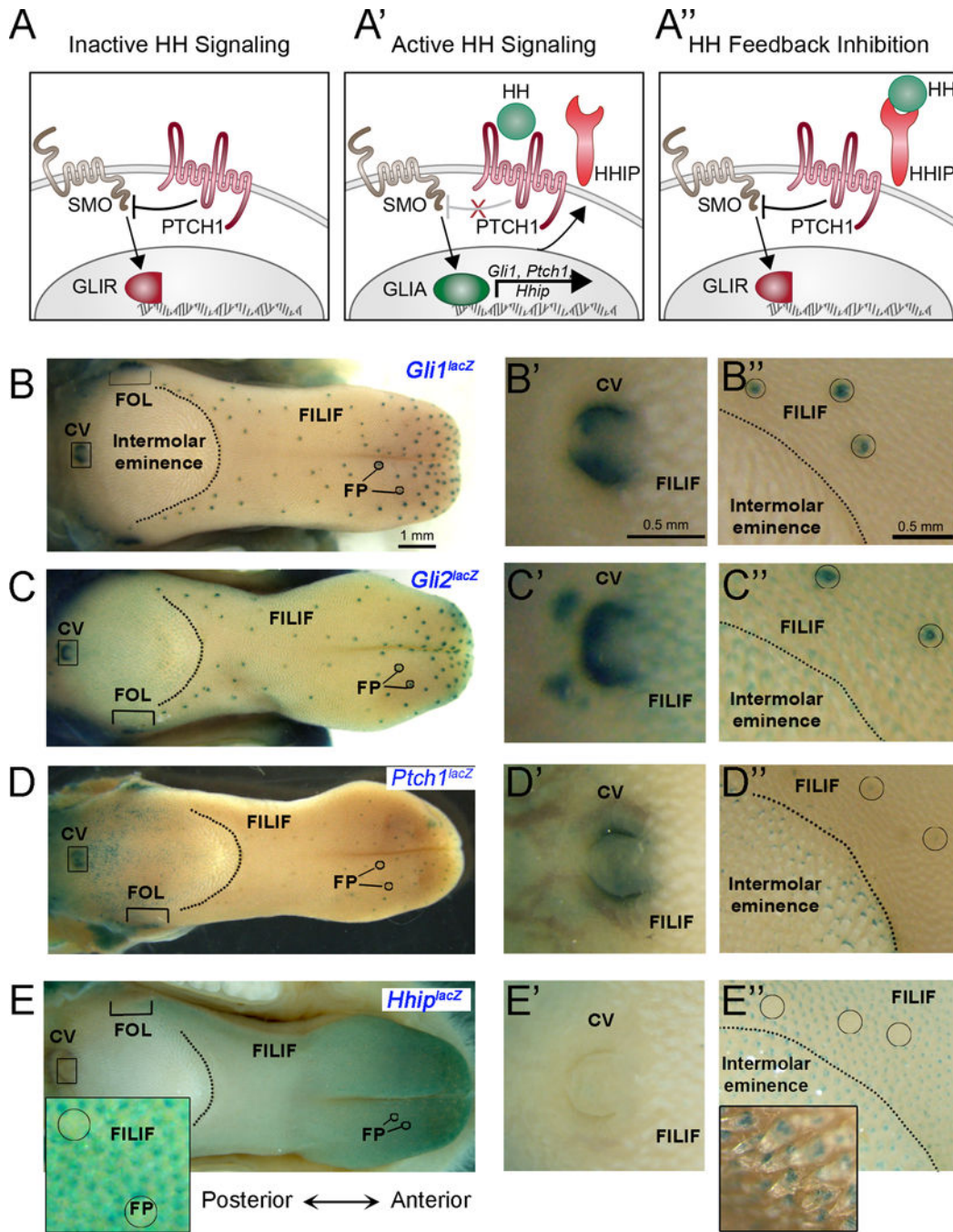


Figure 1. HH pathway component expression in the adult tongue.

(A-A'') Simplified model of HH feedback inhibition. (A) Inactive HH signaling: PTCH1 suppresses SMO in the absence of HH ligand leading to production of GLI repressor (GLIR) and the suppression of HH-dependent gene expression. (A') Active HH signaling: HH ligand binds to PTCH1, relieving SMO inhibition, and leading to GLI activator (GLIA) production and the initiation of HH target gene expression (including *Gli1*, *Ptc1*, and *Hhip*). (A'') HH feedback inhibition: HHIP protein sequesters HH ligand, allowing unbound PTCH1 to re-establish SMO repression, and the subsequent repression of HH pathway activity. (B-E)

X-Gal staining of whole tongues from *Gli1^{lacZ/+}*, *Gli2^{lacZ/+}*, *Ptch1^{lacZ/+}* and *Hhip^{lacZ/+}* mice. (B) *Gli1^{lacZ}* is expressed in all three taste papillae: fungiform (FP, circles) on the anterior tongue, foliate (FOL, bracket) and circumvallate (CV, box, B') on the posterior tongue. The remaining tongue is covered by *Gli1^{lacZ}* negative non-taste filiform papillae (FILIF) on the anterior tongue and on the taste papilla-free intermolar eminence (B''). The scale bars apply to all whole tongue images. (C-C'') *Gli2^{lacZ}* is present in both taste (FP, CV and FOL) and non-taste FILIF papillae. (D-D'') *Ptch1^{lacZ}* expression is apparent in FP, CV and FOL and in FILIF in intermolar eminence. (E-E'') *Hhip^{lacZ}* is expressed in non-taste FILIF in the anterior tongue and intermolar. Insets illustrate expression in FILIF surrounding FP (E) and in the intermolar eminence (E''). Dotted lines demarcate intermolar eminence from anterior tongue.

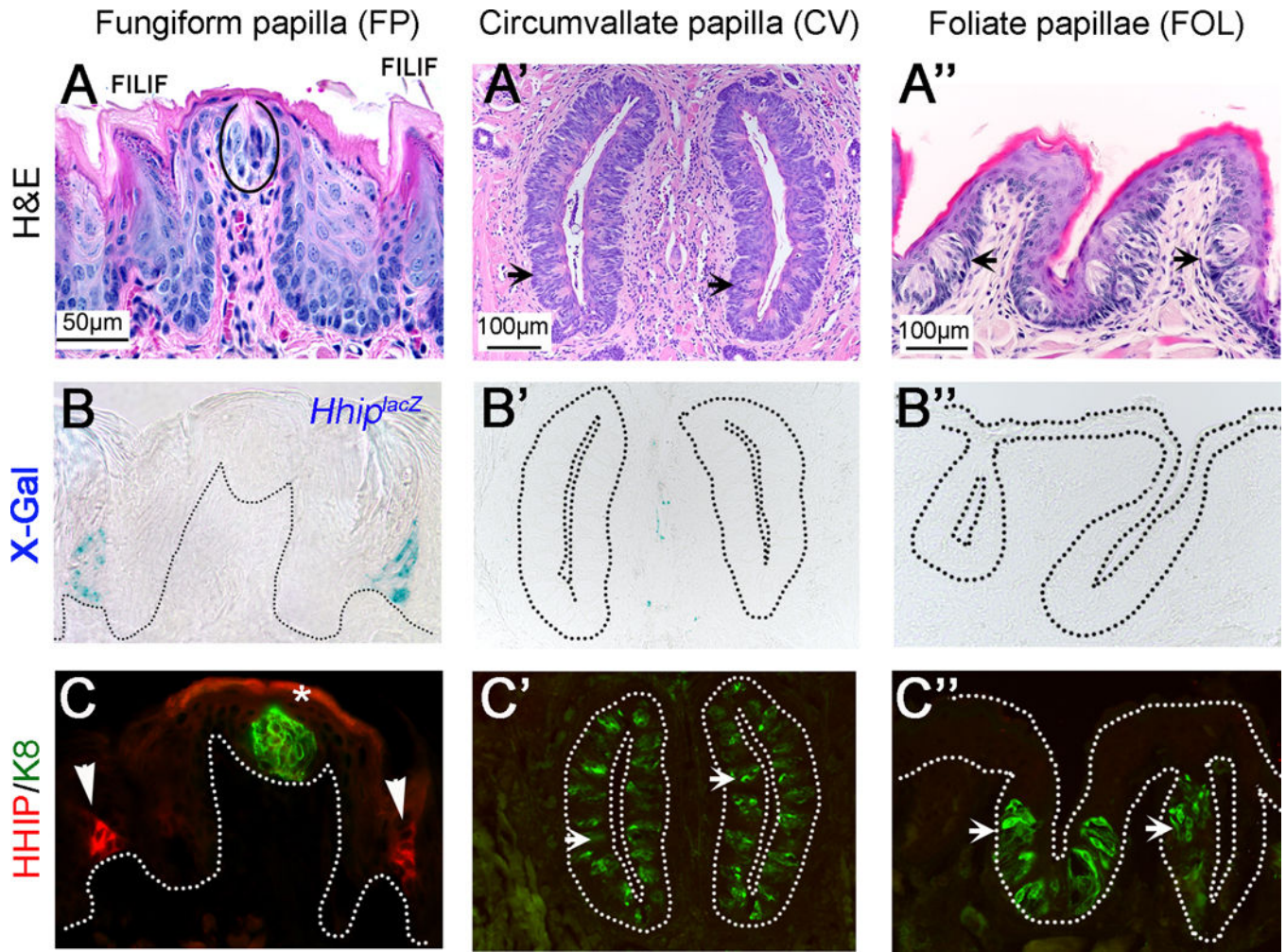


Figure 2. *Hhip* is expressed exclusively in non-taste papillae. (A-A'') H&E staining of FP bracketed with FILIF (A, sagittal section), CV (A', horizontal section), and FOL (A'', horizontal section) in Control tongue to illustrate tissue morphology. The taste bud is indicated by an oval in the FP (A) and arrows in CV (A') and FOL (A''). (B-B'') X-Gal staining (blue) in *Hhip^{lacZ}* tongue sections indicates expression in FILIF only and not in FP (B), CV (B') or FOL (B''). (C-C'') Immunostaining of HHIP (red) and taste bud cells (K8, green) in Control tongue demonstrates protein expression only in FILIF (C, arrow heads) similar to *Hhip*. Arrows mark taste buds in CV (C') and FOL (C''). Dotted lines outline the epithelium. Scale bars in A-A'' apply to corresponding images in B-B'' and C-C''. Asterisk in C denotes non-specific surface staining.

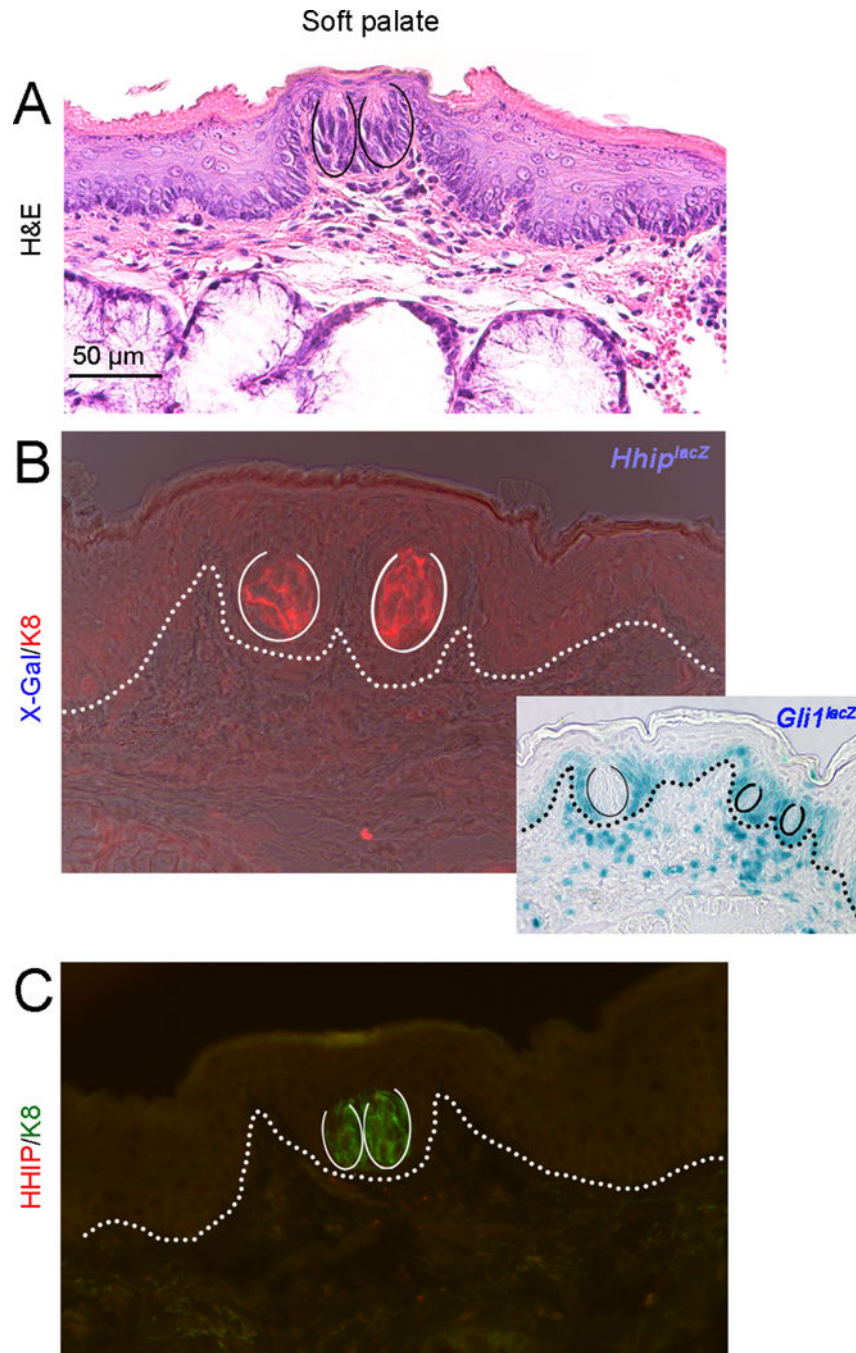


Figure 3. Absence of Hhip gene and protein expression in soft palate.

(A) H&E staining of soft palate (coronal section) in Control tissue to illustrate morphology. (B) X-Gal staining from *Hhip*^{lacZ} reporter mouse indicates no expression in soft palate. Taste buds are labeled by K8 (red). Inset indicates positive *lacZ* expression in soft palate from *Gli1*^{lacZ} reporter mouse. (C) Antibody detection of endogenous HHIP (red) and taste bud cells (K8, green) in Control tongue. There is no HHIP expression in soft palate, similar to absence of *Hhip* gene expression. Taste buds are outlined with oval lines in A-C. Dotted lines in B and C outline the base of the epithelium. Scale bar in A applies to B and C.

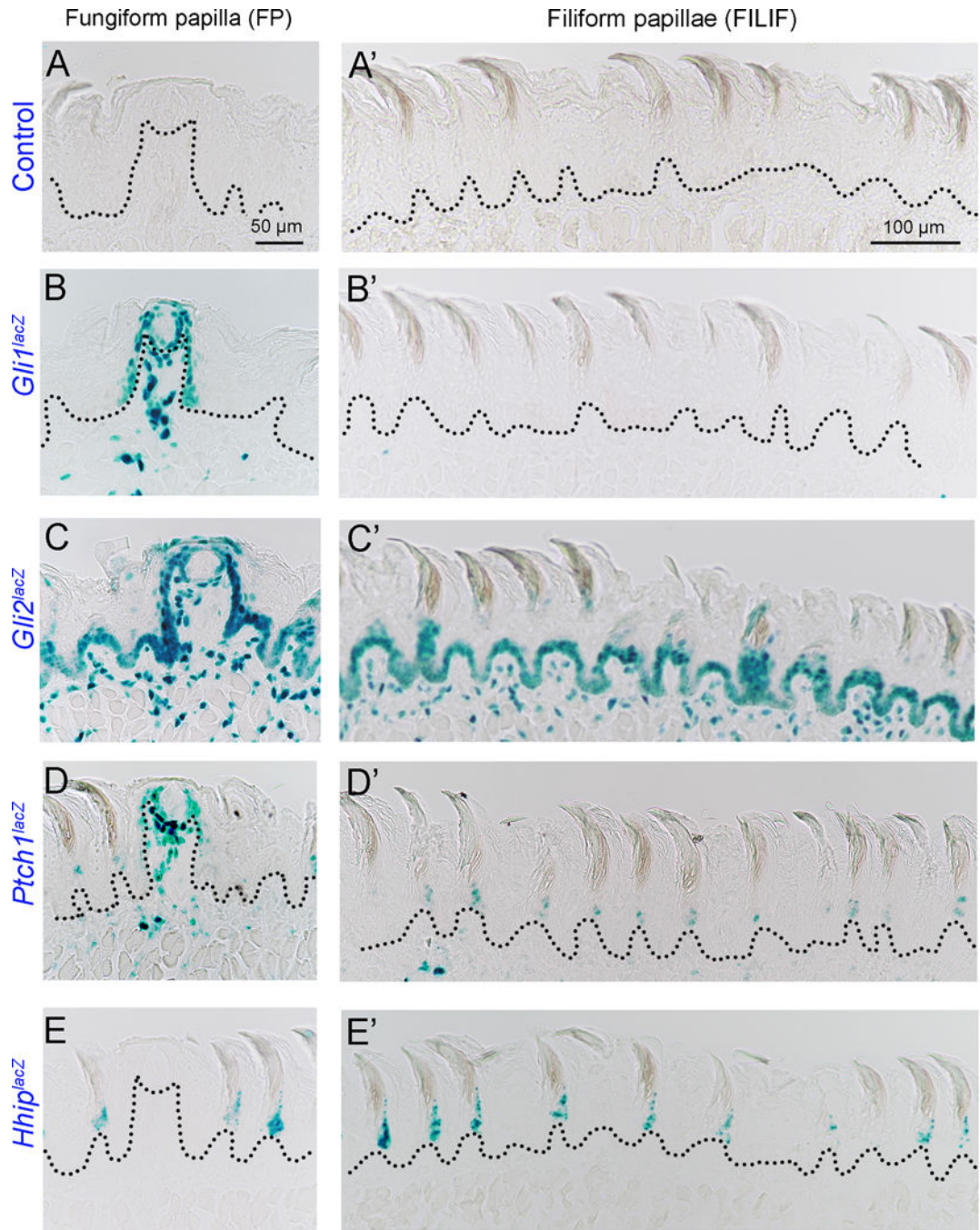


Figure 4. HH pathway component expressions in fungiform and filiform papillae.

X-Gal staining of FP (A-E) and FILIF (A'-E') papillae in sagittal sections from a *lacZ* negative Control mouse and *Gli1^{lacZ}+*, *Gli2^{lacZ}+*, *Ptch1^{lacZ}+* and *Hhip^{lacZ}+* reporter mice. (A,A') There is no X-Gal staining in Control tissue. Scale bars apply to all corresponding images from reporter mice. (B) *Gli1^{lacZ}* cells are observed in basal epithelial cells of the FP walls, in perigemmal and in stromal cells. (B') No *Gli1* expression is detected in FILIF. (C,C') *Gli2^{lacZ}* is expressed throughout the entire basal epithelial and stromal cells of FP and FILIF. (D,D') *Ptch1^{lacZ}* is expressed in FP basal epithelial cells, perigemmal and

stromal cells, and in a subset of FILIF cells. (E,E') Expression of *Hhip^{lacZ}* is observed only in FILIF, in a subset of cells. There is no *Hhip^{lacZ}* expression in FP cells. Black dotted lines outline the base of the epithelium.

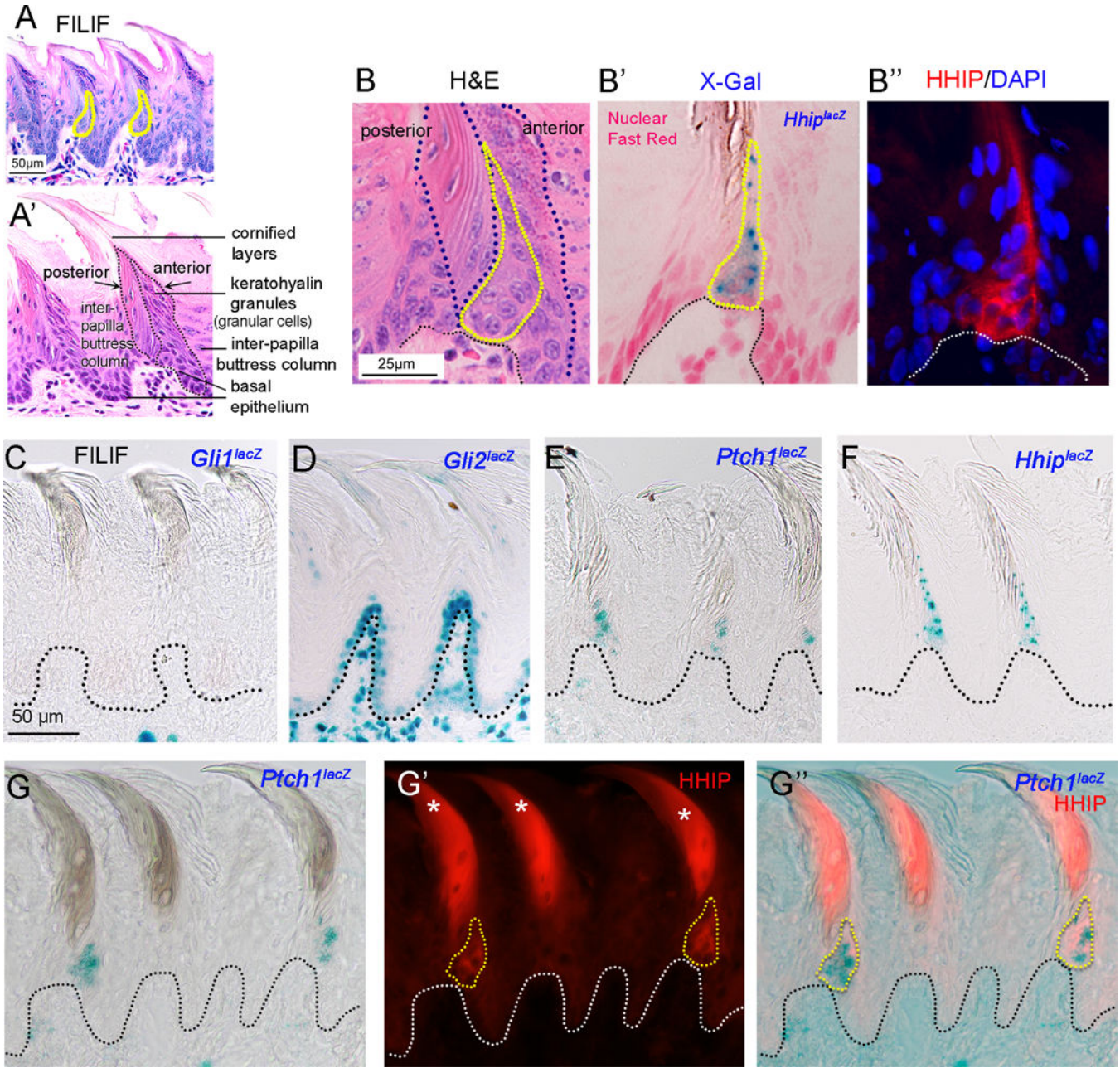


Figure 5. *Ptch1* and *Hhip* are expressed in *Gli*-negative cells in FILIF.
 (A-A') H&E staining of filiform papillae (FILIF) in sagittal sections. Yellow dotted lines indicate location of *Hhip* in FILIF (A). FILIF-specific compartments are labeled (A'). Dotted lines demarcate anterior and posterior columns. Anterior column includes granular cell layers with keratohyalin granules. Between the FILIF is the inter-papilla buttress column. The FILIF are covered by thick cornified layers. (B) H&E: A restricted and distinctive pattern of *Hhip* in the anterior epithelial face of FILIF is illustrated (yellow dotted lines) based on the expression of gene and protein. Blue dotted lines demarcate the anterior and posterior FILIF columns. (B') X-Gal: X-Gal staining (blue) from *Hhip^{lacZ}* tongue reveals expression in a subset of FILIF cells (outlined in yellow). Nuclear fast red is used to

label all cells. (B'') HHIP/DAPI: Immunostaining of HHIP (red) demonstrates an expression pattern and location that directly correspond to *Hhip*. DAPI stains cell nuclei. (C-F) X-Gal staining of FILIF from *Gli1^{lacZ/+}*, *Gli2^{lacZ/+}*, *Ptch1^{lacZ/+}* and *Hhip^{lacZ/+}* reporter mice. (C) *Gli1^{lacZ}* cells are not detected in FILIF. (D) *Gli2^{lacZ}* cells are present in the basal layer of FILIF epithelium. Both *Ptch1^{lacZ}* (E) and *Hhip^{lacZ}* (F) are observed in a subset of FILIF cells. (G-G'') X-Gal staining in *Ptch1^{lacZ}* tongue followed by HHIP immunostaining (red, G') reveals overlapping expression of *Ptch1* and HHIP outlined with yellow dots (G',G''). Asterisks denote non-specific antibody staining after X-Gal reactions in G'. Black/white dotted lines outline the epithelium in all the images in B-G''.

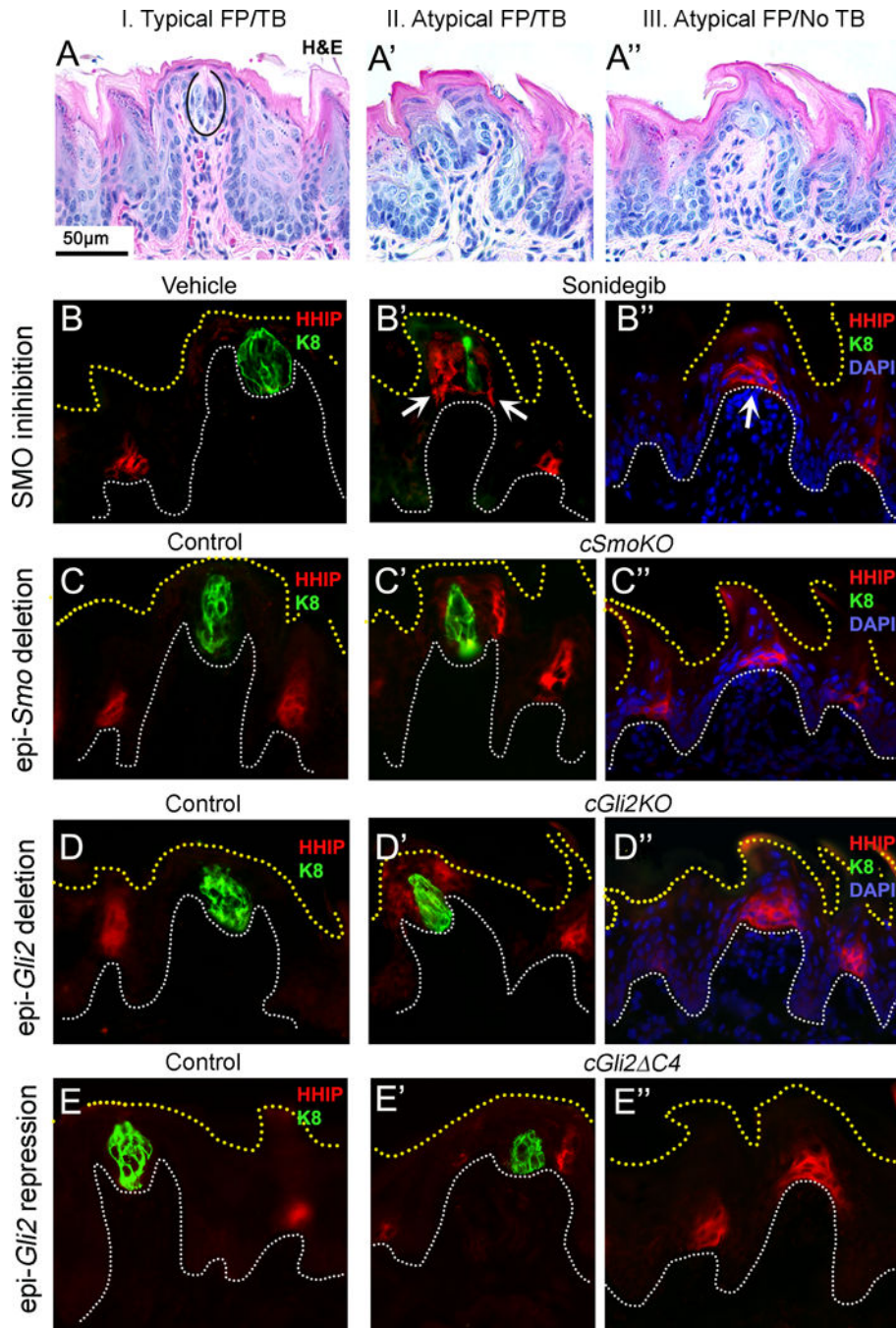


Figure 6. Ectopic expression of HHIP in fungiform papilla after HH pathway inhibition. (A-A'') H&E staining of fungiform papilla (FP)/taste bud (TB, oval outline) to illustrate three categories observed during HH pathway inhibition (HPI): (A) I. Typical FP/TB, (A') II. Atypical FP/TB and (A'') III. Atypical FP/No TB. (B-E) HHIP immunostaining (red) and TB cells (K8, green) after pharmacologic or genetic HPI. (B-B'') HPI targeting *Smo*: SMO inhibition by Sonidegib drug, and (C-C'') epi-*Smo* deletion with epithelial conditional deletion of *Smo* (cSmoKO). In Vehicle and Control, HHIP is consistently observed only in filiform papillae (FILIF) (B,C). After HPI with Sonidegib, in addition to FILIF expression,

ectopic HHIP is observed next to the TB remnant (B', arrows, Atypical FP/TB) and at FP apex in the former TB-bearing location (B'', arrow, Atypical FP/No TB). Parallel ectopic HHIP expression in Atypical FPs (Type II and III) was seen in *cSmoKO* (C-C''). (D-E) *Gli2* suppression models: (D-D'') epi-*Gli2* deletion with epithelial conditional deletion of *Gli2* (*cGli2KO*), and (E-E'') epi-*Gli2* repression by epithelial conditional activation of repressor form of Gli2 (*cGli2^{C4}*). Similar expression patterns are observed in these HPI models compared to *Smo* inhibition or deletion. In Controls, HHIP expression is only in FILIF and not in Typical FP/TB while after *Gli2* suppression, in Atypical FP/TB and Atypical FP/No TB, there is ectopic expression of HHIP in FP apical regions. In B-E'', white dotted lines outline the base of the epithelium. Yellow dotted lines label the surface of epithelium. DAPI stains cell nuclei.

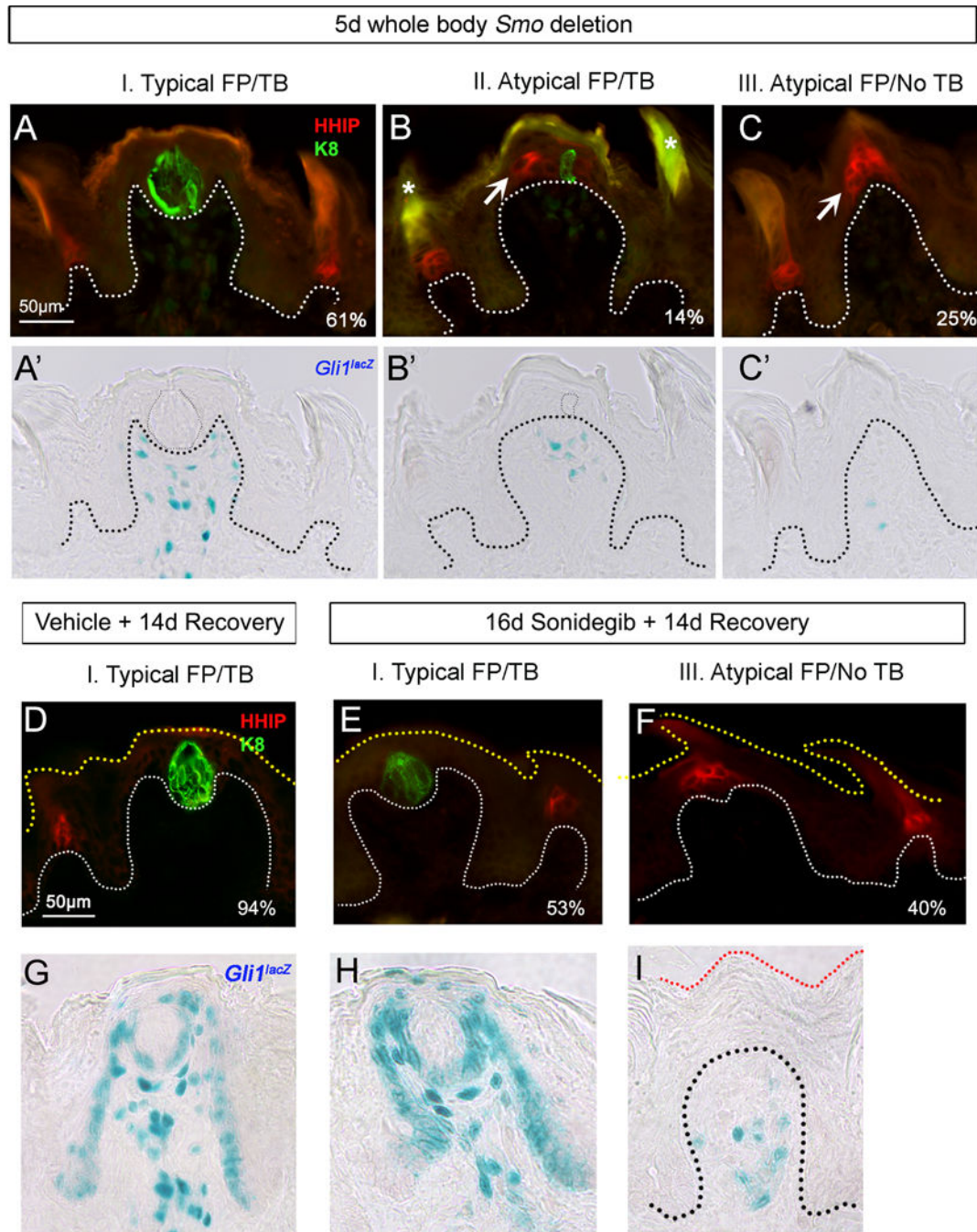


Figure 7. Elimination of *Gli1*+ cells alone after HH pathway inhibition is not sufficient for the induction of ectopic HHIP in fungiform papilla (FP) and expression of ectopic HHIP is not directly impeding FP recovery after withdrawing HH pathway inhibition.

(A-C) Antibody detection of endogenous HHIP (red) and taste bud (TB) cells (K8, green) after 5d whole body *Smo* deletion. Three categories of FP/TB: Typical FP/TB, Atypical FP/TB and Atypical FP/No TB are assessed. Percentage numbers are quantification of the three FP/TB types in a half tongue (total FP = 28). (A'-C') X-Gal staining in the same sections demonstrates elimination of *Gli1*^{lacZ} HH-responding cells from FP basal and perigemmal cell regions in all the three FP/TB types. HHIP expression in Atypical FP with

or without TB (arrows) and *not* in Typical FP/TB suggests a requirement of both SHH and *Gli1* reduction for ectopic HHIP expression. Asterisks in B denote non-specific staining post X-Gal reactions. Dotted lines outline the base of the epithelium. Scale bar in A applies to all images. (D-F) Antibody detection of endogenous HHIP (red) and TB cells (K8, green) after Vehicle and 16d sonidegib treatment followed by 14 days Recovery (discontinuation of drug). Percentage numbers are quantification of Typical FP/TB and Atypical FP/No TB during Recovery from previous findings⁴. There is no HHIP expression in Typical FP/TB in Vehicle (D) or after Recovery (E). Ectopic HHIP expression is apparent in Atypical FP/No TB even after stopping the drug treatment for 14 days (F). (G-I) X-Gal staining in *Gli1^{lacZ}* reporter mouse in Vehicle and Sonidegib treated Recovery group showed usual *Gli1^{lacZ}* expression, in FP basal, perigemmal and stromal cells, in Vehicle (G) and in the recovered Typical FP/TB (H). In Atypical FP/No TB, while *Gli1^{lacZ}* expression is not restored in FP epithelium (I) HHIP expression is maintained at the FP apex (F). Thus, if *Gli1^{lacZ}*⁺ cells are resumed during recovery the ectopic HHIP expression is simultaneously lost, and when there is no *Gli1^{lacZ}* activity HHIP is retained. Dotted lines outline the base of the epithelium. Yellow dotted lines label the surface of epithelium. Scale bar applies to all images.

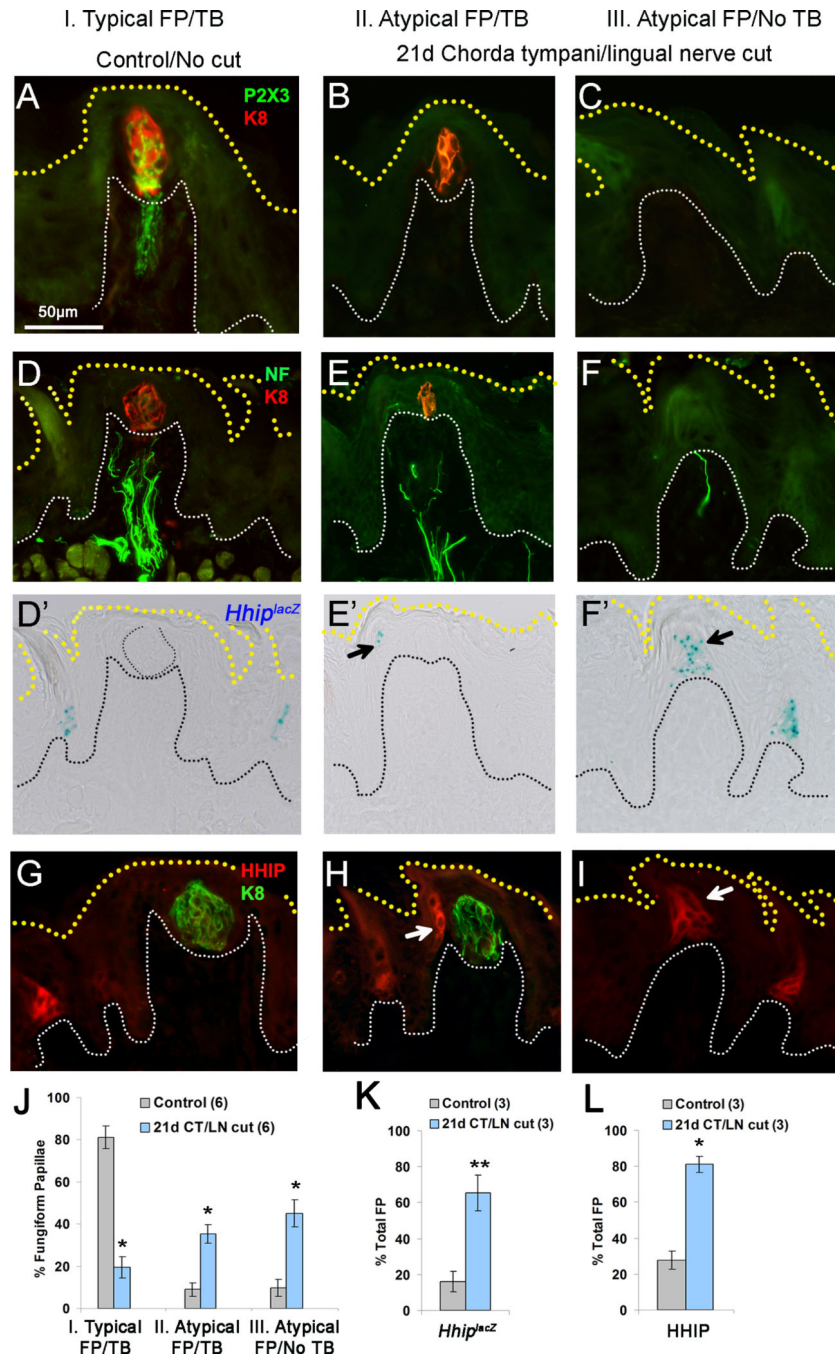


Figure 8. Ectopic expression of Hhip in fungiform papilla after chorda tympani/lingual nerve cut.

(A-F) Immunostaining of the chorda tympani, CT (P2X3, green) and lingual, LN nerves (NF, green), and taste bud cells (K8, red) in Control (no nerve cut) side of tongue and in contralateral tongue after 21 days of CT/LN nerve cut. Three types of fungiform papilla (FP)/taste bud (TB) are assessed: I. Typical FP/TB, II. Atypical FP/TB and III. Atypical FP/No TB. In Control, in Typical FP/TB, the CT nerve innervates TB (A) while the LN nerve is widely distributed to FP epithelial cells (D). After nerve cut, in Atypical FP with or without the TB, the CT nerve is eliminated (B,C) and LN nerve fibers are much

reduced (E,F). (D'-F') X-Gal staining in *Hhip^{lacZ/+}* reporter demonstrates expression in FILIF (Control) in Typical FP/TB and an ectopic expression at/near the FP apical region after the CT/LN nerve cut in Atypical FP/TB and Atypical FP/No TB (arrows). (G-I) HHIP immunostaining (red) resembles *Hhip* expression in Control tongue and in contralateral tongue after CT/LN nerve cut (arrows). K8 labels TB cells (green). Yellow dotted lines label the surface of epithelium in A-I. White dotted lines outline the base of the epithelium in A-I. Scale bar in A applies to the images in B and C. (J) Percentage of Typical FP/TB, Atypical FP/TB and Atypical FP/No TB in Control and CT/LN nerve cut. (K) Percentage of total FP with ectopic *Hhip* expression in *Hhip^{lacZ}* reporter, in Control and after CT/LN nerve cut. (L) Percentage of total FP with ectopic HHIP expression in Control and after CT/LN nerve cut. Statistical analysis is independent sample t-test (* $p < 0.001$; ** $p < 0.01$). Numbers in parentheses are number of animals analyzed.

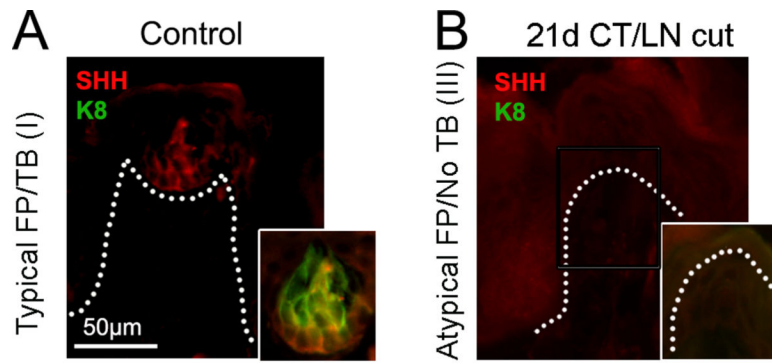


Figure 9. SHH expression after chorda tympani (CT)/lingual (LN) nerve cut. (A) Antibody detection of SHH (red) and taste bud cells (K8, green) in the Control side of tongue, in Typical FP/TB, and (B) in contralateral tongue, in Atypical FP/No TB after 21 days of CT/LN nerve cut. There is loss of SHH in association with loss of TB cells.

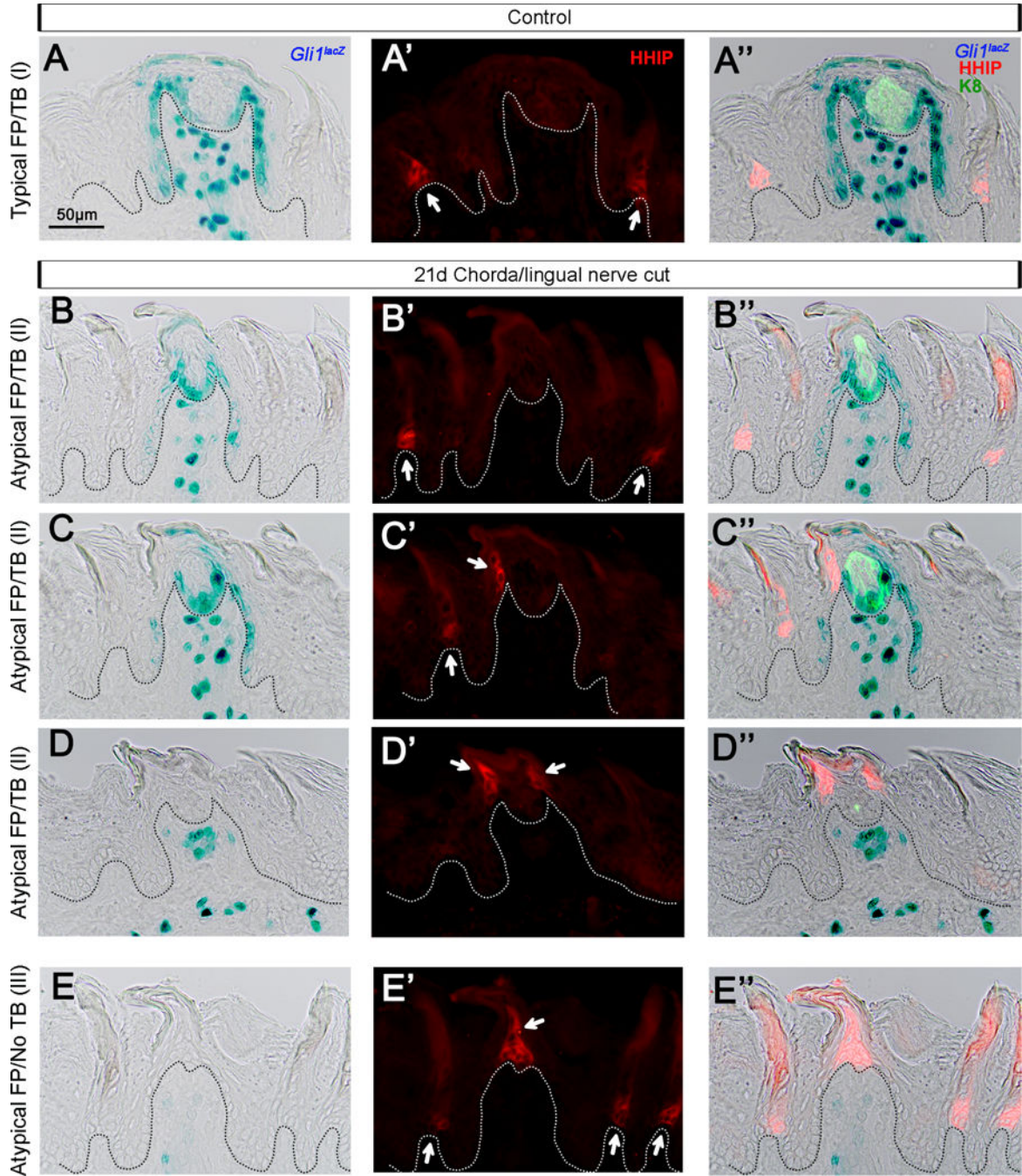


Figure 10. Ectopic HHIP correlates with loss of HH signaling after chorda tympani/lingual nerve cut.

(A) X-Gal staining from *Gli1^{lacZ/+}* reporter in Control Typical FP/TB illustrates HH signaling in FP basal, perigemmal and stromal cells. (A') HHIP immunostaining (red) in the same sections demonstrates expression in FILIF only (white arrows). (A'') Merged images with TB cells (K8, green) indicate absence of HHIP and presence of *Gli1^{lacZ}* in Typical FP/TB. (B-E) After 21 days of chorda tympani (CT)/lingual (LN) nerve cut, X-Gal staining from *Gli1^{lacZ/+}* reporter illustrates graded loss of HH signaling in FP basal and perigemmal cells. (B'-E') HHIP immunostaining (red) in the same sections demonstrates an ectopic

expression at FP apex in addition to the expression in FILIF (white arrows). (B''-E'')

Merged images of *Gli1^{lacZ}*, HHIP and TB cells (K8, green) indicate opposing expression patterns of *Gli1^{lacZ}* and HHIP. (B-D) In Atypical FP/TB three different expression patterns of *Gli1^{lacZ}* and HHIP are observed. (B-B'') *Gli1^{lacZ}* cells are retained in FP walls and there is no HHIP expression. (C-C'') *Gli1^{lacZ}* cells are gradually lost from one side of FP wall and HHIP expression is observed at the FP apex on the same side where *Gli1^{lacZ}* is eliminated. (D-D'') *Gli1^{lacZ}* cells are completely eliminated from FP walls and perigemmal cells, and HHIP ectopically expressed at both sides of FP apex bracketing the TB remnant. (E-E'') In Atypical FP/No TB there are no *Gli1^{lacZ}* cells in FP and acquisition of HHIP in the entire FP apical area.

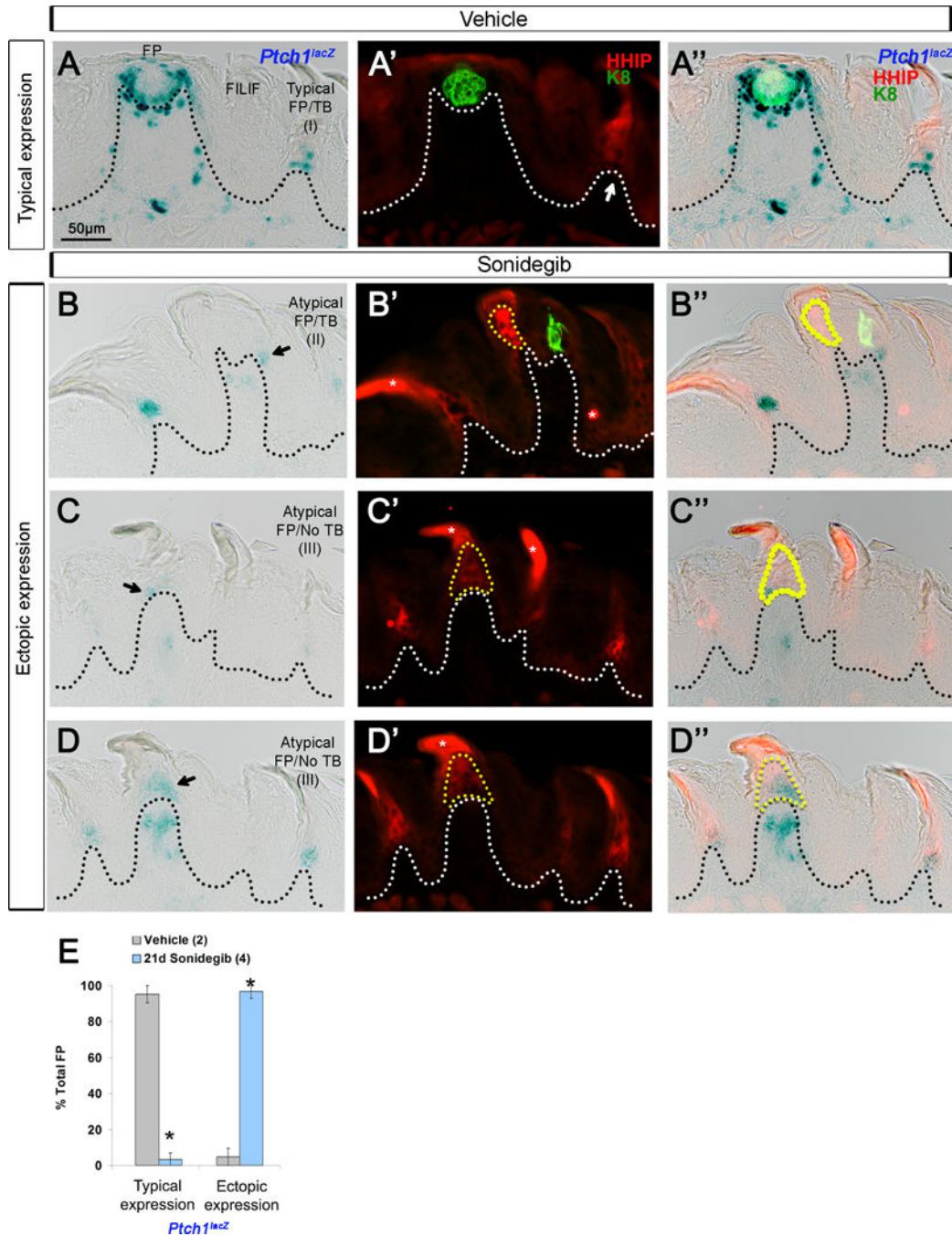


Figure 11. HH-dependent and HH-independent *Ptch1* expression revealed after HH pathway inhibition.

(A) X-Gal staining in *Ptch1^{lacZ/+}* mouse gavaged with Vehicle reveals expression in fungiform papilla (FP) basal, perigemmal and stromal cells and in a subset of filiform papillae (FILIF) cells. (A') HHIP immunostaining (red) and TB cells (K8, green) in the same sections demonstrate HHIP expression in FILIF only (white arrow). (A'') Merged images with *Ptch1^{lacZ}* indicate overlap with HHIP in FILIF. (B-D) After Sonidegib treatment for HH pathway inhibition, X-Gal staining from *Ptch1^{lacZ}* reporter demonstrates retained expression in FILIF while the expression in FP basal and perigemmal cells is lost.

There is remaining *Ptch1^{lacZ}* expression in FP apical basal layer (Atypical FP/TB, black arrows) and an ectopic expression in basal and suprabasal layers at a former TB-bearing location (Atypical FP/No TB, black arrows). (B'-D') HHIP immunostaining (red) and TB cells (K8, green) in the same sections demonstrate ectopic HHIP expression at FP apex (yellow dotted lines). (B''-D'') Merged images of *Ptch1^{lacZ}*, HHIP and K8 indicate partial co-expression pattern of *Ptch1^{lacZ}* and HHIP (yellow dotted lines). Black/white dotted lines outline the base of the epithelium. Asterisks denote non-specific staining post X-Gal reactions. (E) Percentage of total FP with Typical and Ectopic *Ptch1^{lacZ}* expression in Vehicle and after Sonidegib treatment. Statistical analysis is independent sample t-test. (*p<0.001). Numbers in parentheses are number of tongues analyzed.

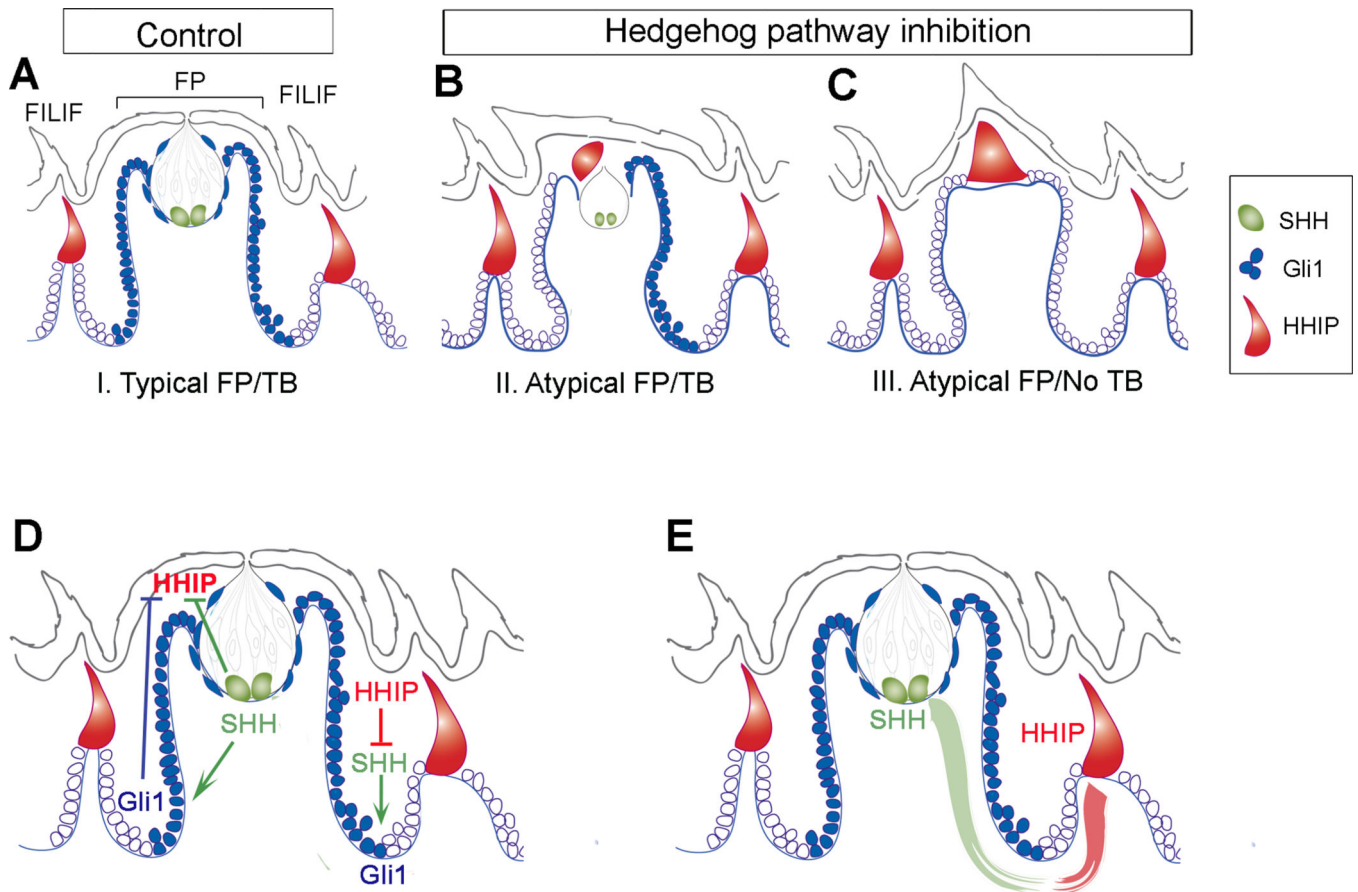


Figure 12. Summary diagrams for HH signaling activity and HHIP expression in Control and after HH pathway inhibition, and models for proposed mechanism of action.

(A-C) HH signaling components in fungiform (FP) and filiform (FILIF) papilla. (A) Control: In Typical FP/TB, SHH ligand (green) is present with the TB basal cells. *Gli1*⁺ HH-responding cells (blue) are in FP basal epithelial and perigemmal cells. HHIP (red) is within FILIF only. Hedgehog pathway inhibition: (B) In Type II Atypical FP/TB there is reduction of SHH⁺ cells from TB, loss of *Gli1*⁺ cells in one side of the FP wall and associated ectopic HHIP expression at the FP apex on the same side as loss of *Gli1*⁺ cells. (C) When *Gli1*⁺ cells are completely eliminated from the FP walls along with loss of SHH in Type III Atypical FP/No TB, ectopic HHIP expression occurs in the FP apex in a location previously occupied by the TB. The FP has acquired a conical FILIF-like morphology. (D) In a proposed mechanism of action: In FP, SHH directly and/or indirectly via activating *Gli1*⁺ cells inhibits HHIP expression in the papilla. In FILIF, HHIP blocks expression of SHH and downstream *Gli1* activity. (E) We propose that the SHH ligand is secreted along FP basal epithelial cells signaling to *Gli1*⁺ cells of the FP wall. Concurrently, HHIP from a FILIF cell subset is secreted along basal epithelial cells and inhibits HH signaling. At the rete peg region of the FP/FILIF epithelia, signaling via *Gli1*⁺ cells is inhibited.